Grace X. Gu[1]
Laboratory for Atomistic and Molecular
Mechanics (LAMM),
Department of Civil and Environmental
Engineering;
Department of Mechanical Engineering,
Massachusetts Institute of Technology,
77 Massachusetts Avenue,
Cambridge, MA 02139

Isabelle Su[1]
Laboratory for Atomistic and Molecular
Mechanics (LAMM),
Department of Civil and Environmental
Engineering,
Massachusetts Institute of Technology,
77 Massachusetts Avenue,
Cambridge, MA 02139

Shruti Sharma
Laboratory for Atomistic and Molecular
Mechanics (LAMM),
Department of Civil and Environmental
Engineering;
Department of Materials Science and
Engineering,
Massachusetts Institute of Technology,
77 Massachusetts Avenue,
Cambridge, MA 02139

Jamie L. Voros
Laboratory for Atomistic and Molecular
Mechanics (LAMM),
Department of Civil and Environmental
Engineering;
Department of Aeronautics and Astronautics,
School of Architecture and Planning,
Massachusetts Institute of Technology,
77 Massachusetts Avenue,
Cambridge, MA 02139

Zhao Qin
Laboratory for Atomistic and Molecular
Mechanics (LAMM),
Department of Civil and Environmental
Engineering,
Massachusetts Institute of Technology,
77 Massachusetts Avenue,
Cambridge, MA 02139

Markus J. Buehler[2]
Laboratory for Atomistic and Molecular
Mechanics (LAMM),
Department of Civil and Environmental
Engineering,
Massachusetts Institute of Technology,
77 Massachusetts Avenue,
Cambridge, MA 02139
e-mail: mbuehler@mit.edu

Three-Dimensional-Printing of Bio-Inspired Composites

Optimized for millions of years, natural materials often outperform synthetic materials due to their hierarchical structures and multifunctional abilities. They usually feature a complex architecture that consists of simple building blocks. Indeed, many natural materials such as bone, nacre, hair, and spider silk, have outstanding material properties, making them applicable to engineering applications that may require both mechanical resilience and environmental compatibility. However, such natural materials are very difficult to harvest in bulk, and may be toxic in the way they occur naturally, and therefore, it is critical to use alternative methods to fabricate materials that have material functions similar to material function as their natural counterparts for large-scale applications. Recent progress in additive manufacturing, especially the ability to print multiple materials at upper micrometer resolution, has given researchers an excellent instrument to design and reconstruct natural-inspired materials. The most advanced 3D-printer can now be used to manufacture samples to emulate their geometry and material composition with high fidelity. Its capabilities, in combination with computational modeling, have provided us even more opportunities for designing, optimizing, and testing the function of composite materials, in order to achieve composites of high mechanical resilience and reliability. In this review article, we focus on the advanced material properties of several multifunctional biological materials and discuss how the advanced 3D-printing techniques can be used to mimic their architectures and functions. Lastly, we discuss the limitations of 3D-printing, suggest possible future developments, and discuss applications using bio-inspired materials as a tool in bioengineering and other fields.
[DOI: 10.1115/1.4032423]

Keywords: 3D-printing, biological materials, bio-inspired materials, functional design, additive manufacturing, composites

1 Introduction

Bio-inspired materials research shows that natural materials, oftentimes made up of biopolymers and minerals, can offer functionalities superior to that of its synthetic counterparts [1]. Previous studies have pointed out that the superior performance of biomaterials strongly depends on their hierarchical structures

---

[2–5]. For example, nacre, which is made up mostly of a hard platelet phase and a small amount of soft biopolymer phase, has a toughness value that is far greater than the hard platelet phase alone [2]. The spider silk, with its unique molecular protein structure and nonlinear material behaviors, allows it to be strong enough to withstand the weight of the spider and prey and extensible enough to absorb energy from impact and environmental factors, including significant wind loading [6]. However, the limitation of the availability and the intrinsic difficulty of harvesting many such materials in large quantities, such as spider silk, make it challenging to use directly for engineering applications. Therefore, it is critical to use alternative ways of designing and producing composites that have material functions similar to their natural counterparts for large-scale applications.

Even though nature provides optimized templates of structures for enhanced material performance, their hierarchical features go beyond the capability of conventional manufacturing methods. We need to develop new ways to build on them and construct them with our own toolbox (Fig. 1). Taking inspiration from architectures found in nature, engineers are optimizing designs to tune mechanical properties of materials. The construction of the complex geometries found in nature is only now possible by combining additive manufacturing techniques, such as 3D-printing, with advanced chemical and biological synthesis methods to make novel inks to print synthetic materials that mimic constituents found in nature. Viscoelastic inks that can be 3D-printed in a layer-by-layer assembly can be made of hydroxyapatite (HA) for engineering bone or silk fiber to make intricate geometries. As a result, the advent of multimaterial 3D-printing allows for the engineering of biologically inspired composite structures such as nacre, bone, hair, and silk for lightweight architecture with enhanced properties such as strength and toughness [7–10].

By developing 3D-printing techniques to manufacture designs found in nature, it will be possible to make materials and structures that are not only optimized for a specific function, but also produced concurrently and with varying architectures across multiple length-scales. Bio-mimicry has already benefited fields such as architecture, engineering, materials science, and medicine. With 3D-printing as a manufacturing tool, we can fabricate more complex customized designs that use several materials and distinct geometries that previously could not be engineered. Through the 3D-printing of synthetic spider silk, flexible yet durable sutures can be made to enhance integration of medical implants [11]. Common materials that are usually brittle such as aragonite and HA could be printed in geometries that tune their mechanical properties to increase elasticity [12]. 3D-printing can help mimic architectures to create tougher structures, like those found in nacre to make stronger buildings that can withstand natural disasters and extreme environmental conditions. Biomimicry using 3D-printing can also improve conservation and collection of renewable energy [13]. For example, designs of blades of wind turbines inspired by fins, tails, and flippers are expected to increase the annual electrical production by 20% [14]. Taking inspiration from nature to influence 3D-printing of structures will help us in overcoming limitations in medicine, renewable energy, engineering, and many more fields.

The plan of the paper is as follows. Section 2 discusses a variety of interesting biomaterials with regard to their structure, function, and building blocks. These include bone, nacre, silk, and hair. Section 3 describes the current state of 3D-printing, including the advantages, the different types, material innovations, and resolution. Sections 4–6 discuss case studies of 3D-printing of bio-inspired composites, printing of biological structures for functional designs, and limitations of 3D-printing.
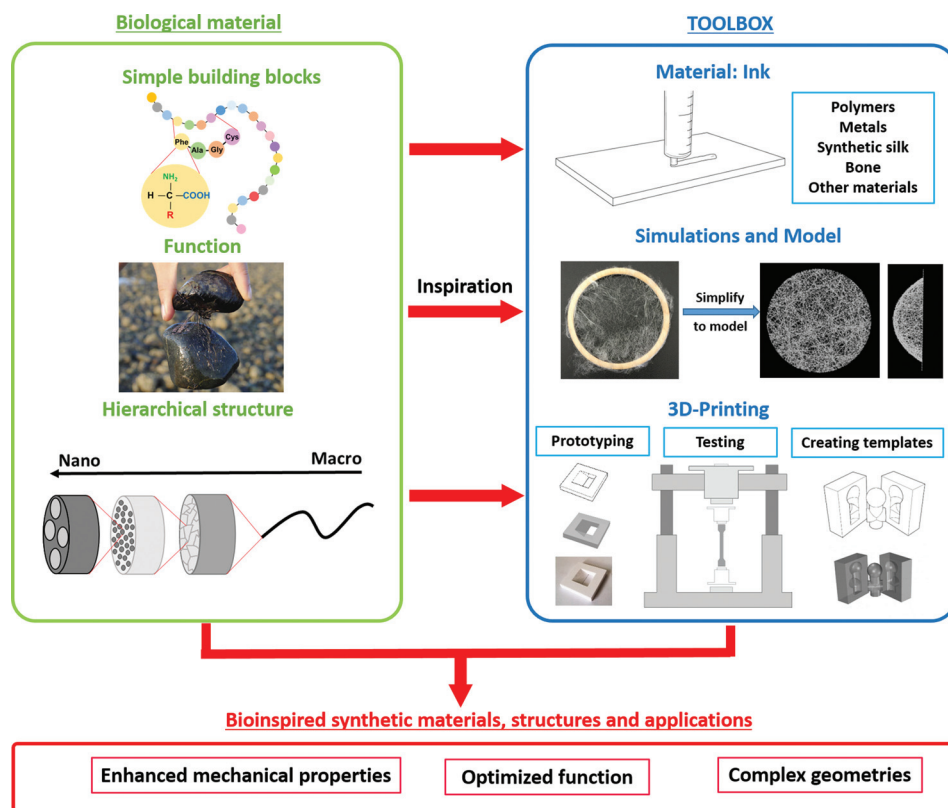

Fig. 1 Illustration of design process of bio-inspired synthetic materials, structures, and applications through the interaction between biological materials and 3D-printing. Biological materials are optimized through evolution and are an inspiration for scientists and engineers. 3D-printing together with modeling has become an efficient predictive tool to understand nature and create improved bio-inspired synthetic materials.
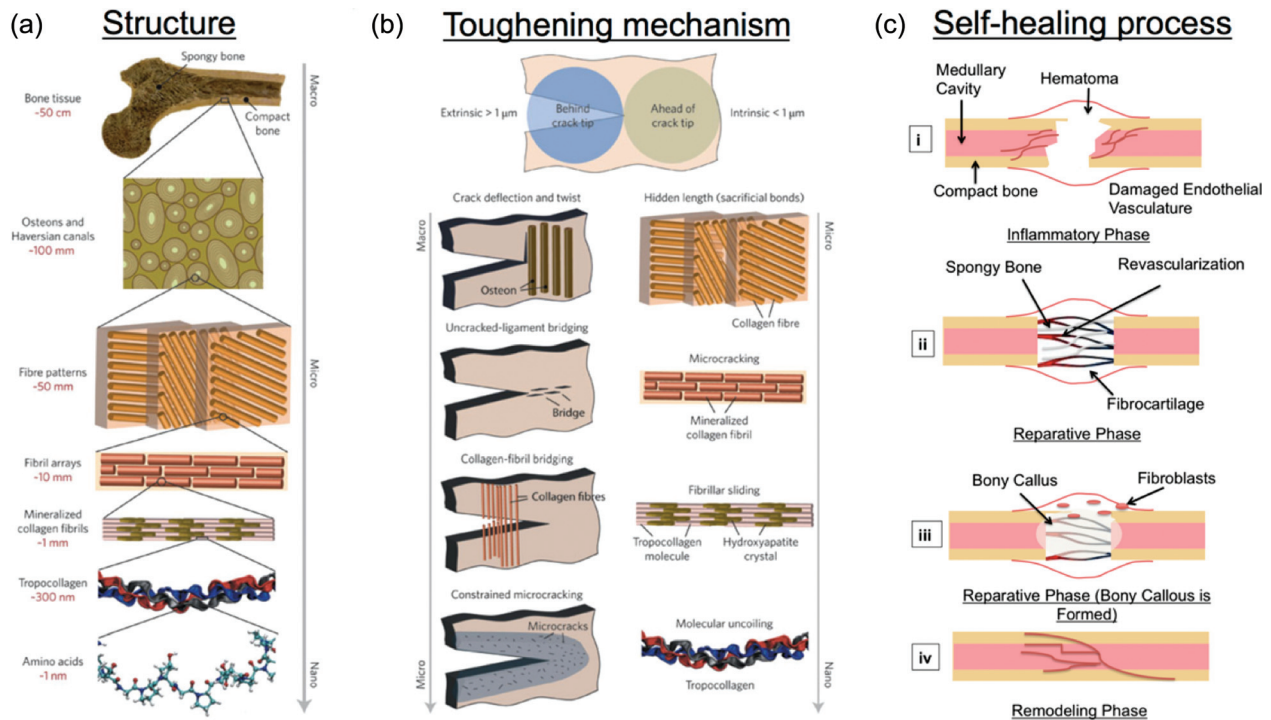
Fig. 2 (*a*) Biological bone's seven levels of hierarchy from the nanoscale to macroscale. Adapted from Launey et al. [15]. Copyright 2010 by Annual Reviews. (*b*) Toughening mechanisms of bone include molecular uncoiling, fibrillar sliding, and microcracking on the smaller scales, and the larger scales include collagen–fibril bridging, uncracked-ligament bridging, and crack deflection. Adapted from Launey et al. [15]. Copyright 2010 by Annual Reviews. (*c*) Self-healing process of bone includes: inflammatory response, repair stage, and the remodeling stage.

Section 7 provides a summary and discusses the future direction of 3D-printing of bio-inspired materials, including scaling up, commercialization, multiple materials, and ways to improve the printing process. For this paper, we acknowledge omission of the challenges in ink chemistry development; however, if the reader is interested, discussion on ink chemistries can be found in Ref. [8].

2 Biological Materials

2.1 Bone. Bone performs incredibly in terms of stiffness and toughness due to the hierarchical organization of the organic and inorganic materials that interact from the nanoscopic scale (Fig. 2(*a*)). Mechanical properties of cortical bone and various other biomaterials are shown in Table 1. On the nanoscopic scale, collagen molecules and mineral platelets form collagen fibrils [15,24]. These fibrils make up fiber bundles on the micrometer scale. Fiber bundles are organized in lamellae within osteons on the centimeter scale [4,24]. Osteons are cylindrical structures found in compact bone, the other type being cancellous bone. Various toughening mechanisms found in bone structures make it a very unique and tough material worthy of studying. Large number of interfaces that exists on the fibrous lamellar structure of bone result in toughening mechanisms such as crack-bridging, microcrack formation, and crack deflection [25], as shown in Fig. 2(*b*).

Another feature in lamellar bone is its highly anisotropic nature in its stiffness, strength, and fracture toughness, which allows it to dissipate energy [15,26,27]. There are orders of magnitude differences in energy dissipation depending on the direction of crack propagation, whether it is perpendicular or parallel to the lamellae [15,26].

In addition to its superior toughening mechanisms, bone and most body organs are capable of being repaired and healed by themselves after being damaged. In general, they demonstrate the ability to recover functionality using the resources inherently available to them. Biological bones typically have a three-step process to self-healing, which includes: inflammatory response (immediate), reparative stage (secondary), and matrix remodeling (long-term) [28], as shown in Fig. 2(*c*). During the reparative phase, dying osteocytes, damaged periosteum and marrow are resorbed, and pluripotent mesenchymal cells begin to form fibroblasts, chondroblasts, and osteoblasts. The *p*H becomes neutral and then slightly basic to allow alkaline phosphatase activity for mineralization of the callus. At the end of the reparative phase, there is much cartilage overlaying the fracture site and calcification begins via endochondral ossification [29]. The final phase is the remodeling phase and begins with replacement of the woven bone via osteoclastic resorption of poorly located trabeculae, formation of new bone along lines of stress, and resorption of excess callus [30]. In reversal, mononuclear cells migrate to the surface of the bone, and

Table 1 Material properties of various biomaterials [15–23]. RH is relative humidity

Material	Young's modulus (GPa)	Tensile strength (MPa)	Strain to failure (%)	Compressive strength (MPa)	Fracture toughness (MPa $\sqrt{m}$)	Work of fracture (M J m^{-3})
Cortical bone	7–30	50–150	1–3	30	2–12	—
Abalone Nacre	25–90	78	1–8	250–700	4.5–10	—
Araneus MA silk	10	1100	27	—	—	160
Bombyx mori cocoon silk	7	600	18	—	—	70
Wool, 100% RH	0.5	200	50	—	—	60
Hair	3.3	117	35	—	—	—

in formation, osteoblasts place new bone until resorbed bone is completely replaced. The remodeling phase of the bone enables the new bone to mimic the architecture of the old bone to meet changing mechanical needs of the skeletal system [31].

2.2 Nacre and Other Hybrid Materials. Natural materials including nacre, barnacle, and abalone have outstanding mechanical functions for resisting impacts and tolerating defects because of the unique way they bring two different materials together at the nanoscopic scale [32,33]. Their material functions are superior to any of their single material phases, inspiring several hybrid composite materials made of inferior building blocks [32]. The idea of hybrid materials has allowed designers to use several different materials as building blocks and achieve multiple material functions and applications by altering the ratio and architecture of how they combine for a specific function and application [32]. Similarly, different natural materials employ two vastly different materials to achieve a specific function for survival [34–36]. Here, we discuss various hybrid materials seen in nature that employ soft and stiff building blocks that helps to explain their superior mechanical properties.

Nacre is a hierarchical natural composite consisting of platelets of calcium carbonate glued together by a biopolymer (Fig. 3(a)).

Nacre mostly consists of mineral; however, its toughness is orders of magnitudes above that of the pure mineral materials. Part of the reason for this is its brick and mortarlike arrangement of aragonite platelets, which shows a unique architecture when compared to traditional engineering materials [2,4,16,40,41]. Its toughness can originate from a few possible toughening mechanisms [17,25,42–45]. First, due to the large number of interfaces between mineral platelets, cracks are deflected as they propagate. Other toughening mechanisms can include crack bridging, friction between nano-asperities, and plate pullout, which increases energy dissipation leading to increased toughness. In addition, nacre's unique brick and mortar architecture allows it to have anisotropic mechanical properties [26]. Nacre's weakest direction is tension perpendicular to the direction of the mineral bricks and its strongest direction is compression perpendicular to the direction of the mineral bricks (Fig. 3(b)). This knowledge reveals the potential strength of nacre's design when it comes to pressurized environments. Applications for which materials need to endure highly pressurized environments can benefit from nacre's anisotropic structure. One example is an underwater container or vehicle, which needs to be submerged under water for long time and obtain long depths under water, subjecting to compressive stress from its surrounding environments. One thought is that with a
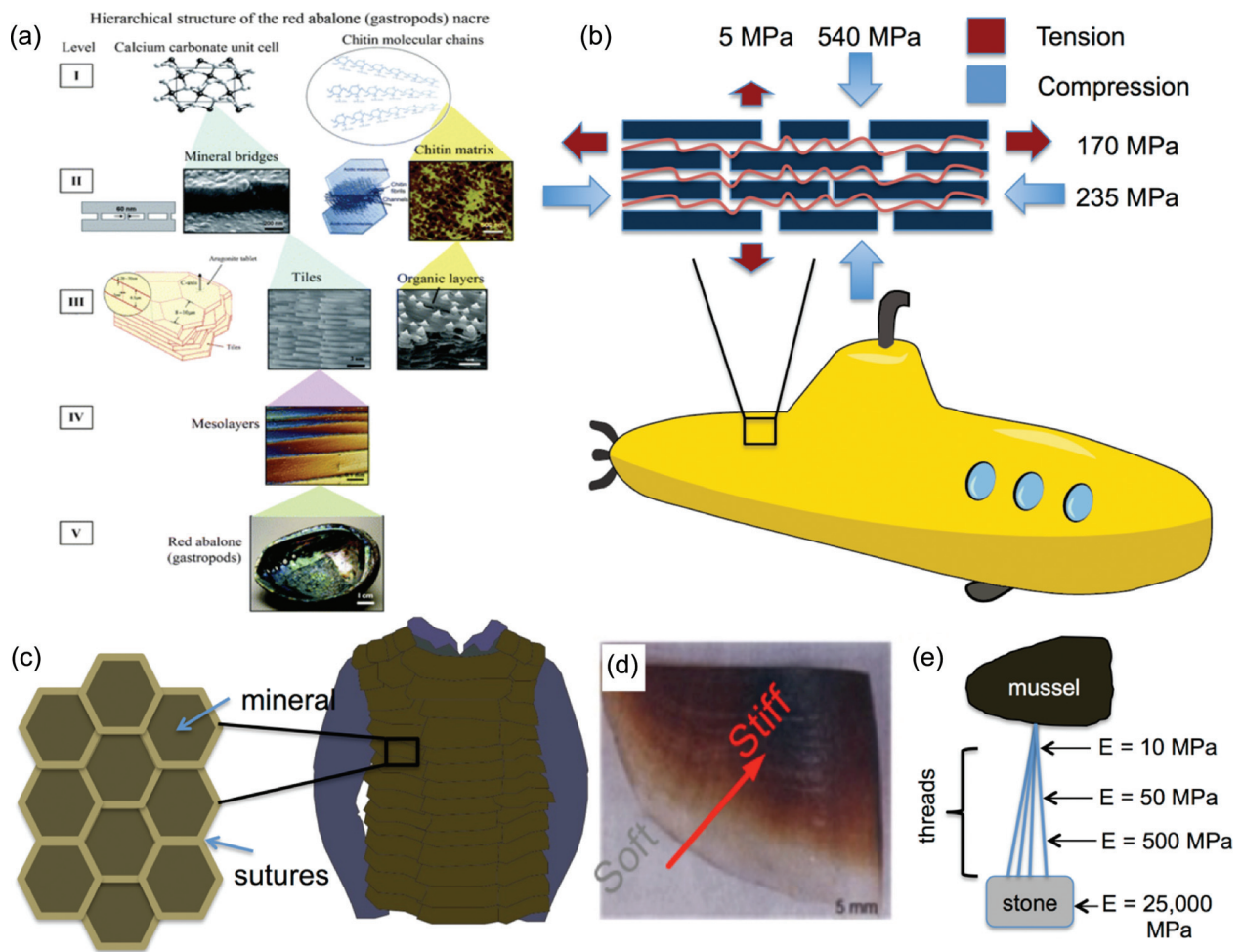

Fig. 3 (a) Hierarchical structure of red abalone from nano-, to micro-, to meso-, to macroscales. Reproduced with permission from Sun and Bhushan [20]. Copyright 2012 by The Royal Society of Chemistry. (b) Nacre has different compressive and tensile strengths under different loading directions [37]. Nacre's anisotropic nature allows it to endure high compressive forces, which can be beneficial for underwater designs such as a submarine. (c) Turtle shell architecture allows the shell to be flexible at small strains and strong in high strains, which can help improve protection designs. (d) Tensile stress–strain curve for different parts of the squid beak wing. The tensile stress decreases along the compositional gradient from highest being heavily tanned to the lowest being untanned parts. Reproduced with permission from Miserez et al. [38]. Copyright 2008 by The American Association for the Advancement of Science. (e) Schematic showing attachment of a submarine mussel to a stone via the mussel byssus. The proximal part (50 MPa) is more elastic and the distal part (500 MPa) is stiffer [39].

tailored design similar to nacre's, submarines can explore deeper into the water without the concern of early failure, shown in (Fig. 3(b)).

Another example of a hybrid material is silica compound produced by deep-sea glass sponges. Spicules give structural stability to the sponge body, help fend away predators, and transmit light similar to optic fibers. Silica spicules of deep sea sponges are built by concentric layers of silica joined by a glue based on a protein; this multilayered structure reduces crack propagation in the glass [4,26]. There exists a periodic variation of Young's modulus that helps to reduce crack propagation. The toughness of layered silica is boosted because there is a significant variation of modulus between the glass layers and the organic phase in between. In addition, there exists yielding of the organic matrix in shear between the layers that help to blunt crack tips and reduce the material's brittleness. This hybrid combination of soft and stiff materials increases the toughness in silica. In addition to its mechanical property advantages, silica spicules are shown to be multifunctional and carry light, and thereby add another functional aspect. For instance, Brummer et al. have studied the siliceous

light transmission system in sponges [46]. Additionally, they have shown that spicules can transmit light into deeper tissue region and that sponges have a light transmission system that can harbor photosynthetically active microorganisms in deeper tissue regions [46].

The turtle shell itself is a protective structure that needs to be stiff, strong, and tough. However, it also needs to have locomotion and respiration, which means that it needs to be flexible at small strains. Turtle shell has a combination of ribs, which are hard materials and also a soft tissue layer in between the ribs [26,47,48]. The flexibility of this structure comes from the architecture of the suture between each rib. When the deformation is large, the bone fingers on each side of the suture touches, which increases the mechanical protection of the animal. This intricate construction allows for the turtle to have flexibility at low strains and high stiffness at large strains [26]. We could perhaps apply such design towards the protection armor that needs to have flexibility for mobility but at the same time strong enough to shield humans from being attacked. Although such idea has been applied to many different kinds of ancient armors as shown in Fig. 3(c),
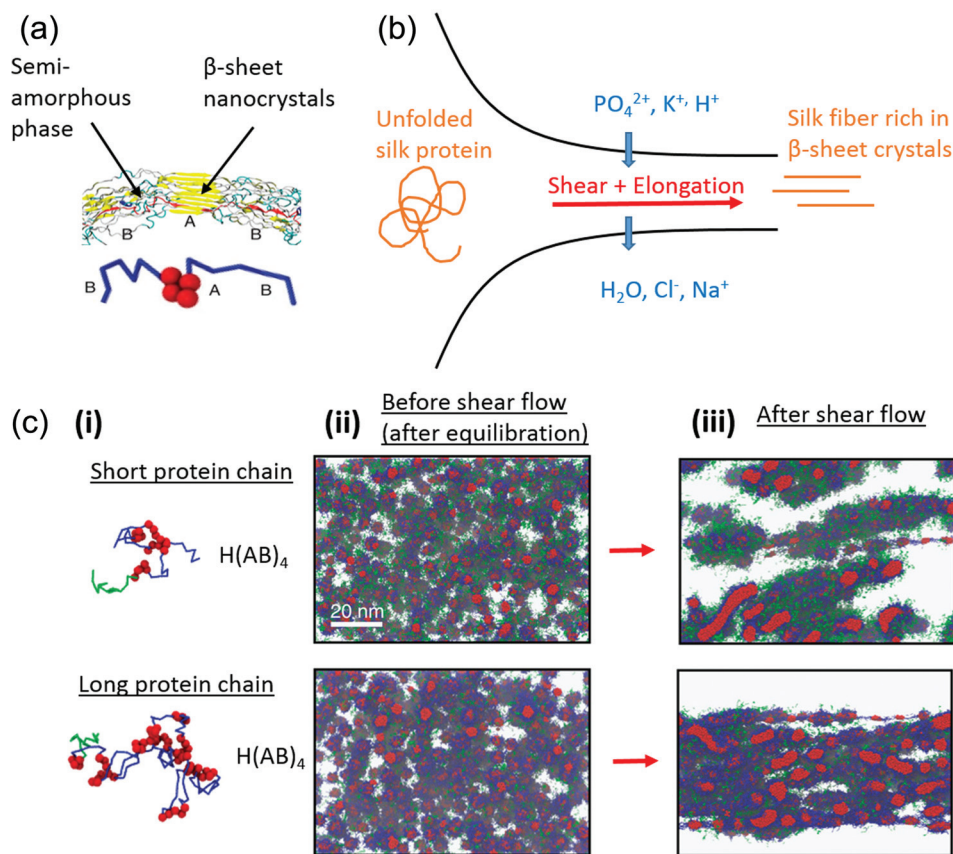

Fig. 4 Analysis of the influence of spinning process and protein chain length on the formation of continuous and robust silk fibers. (*a*) Synthetic silk protein model and main building blocks. Building block named "A" represents poly(alanine) and the hydrophobic domain. Building block named "B" represents GGX (X = R, L, Y, or Q) rich and the hydrophilic domain. Hydrophobic A domain forms β-sheet crystals for stiffness and strength. Hydrophilic B domain forms the semi-amorphous phase for extensibility of the silk fiber. Adapted from Lin et al. [58]. Copyright 2015 by Nature Publishing Group. (*b*) Schematic of the natural spinning process. A highly concentrated unfolded protein solution flows through the spinning duct and undergoes shear flow and elongation. The *p*H decreases, and the spinning dope is subjected to ion exchange: phosphate and potassium ions are added while water, sodium, and chloride ions are extracted. The produced silk is aligned and rich in β-sheet crystals. (*c*) Influence of shear flow and protein chain length on the formation of silk fibers. Adapted from Lin et al. [58]. Copyright 2015 by Nature Publishing Group. (i) Single protein snapshot for H(AB)$_4$ (short protein chain) and H(AB)$_{12}$ (long protein chain). Building block named "H" is introduced for purification and is hydrophilic. H(AB)$_4$ and H(AB)$_{12}$ results after equilibration (before shear flow). (ii) H(AB)$_4$ and H(AB)$_{12}$ results after equilibration (before shear flow). (iii) H(AB)$_4$ and H(AB)$_{12}$ results after shear flow.
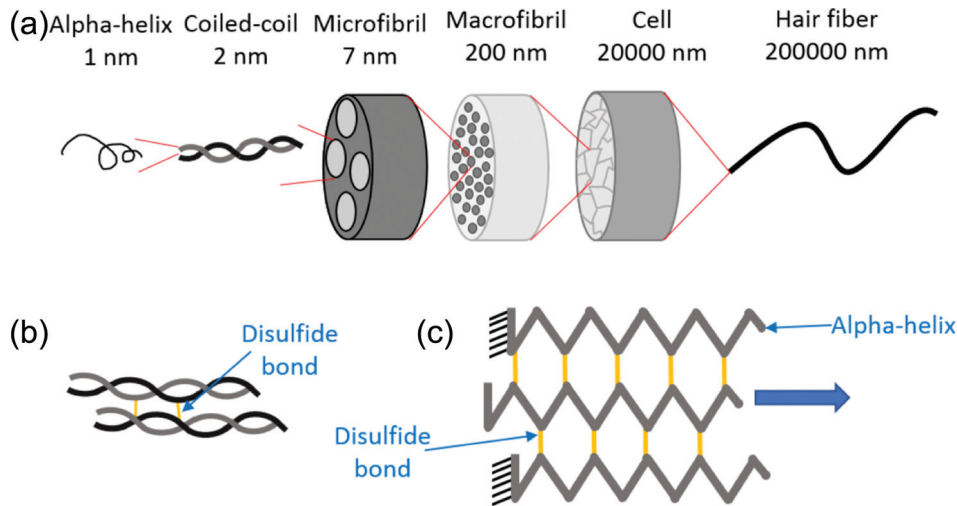
Fig. 5 (*a*) *Hierarchical structure of human hair.* (*b*) Schematic of hair fiber coiled–coil protein composed of alpha-helices, connected by disulfide bond. (*c*) Schematic of a three-strand model composed of three alpha-helices connected by a cluster of disulfide bond with different geometric arrangement and strength.

with the availability of 3D-printing and new materials of lower density and higher strength, we expect to significantly improve the design.

Gradient designs make biological materials strong and tough to survive severe natural forces. In gradient structures, there exists a systematic change in microstructure along the depth on a macroscopic scale. Usually, gradient materials consist of a layered structure where there is a varying layer composition along one axis [39]. In nature, gradient biomaterials are often used to connect soft tissues to a stiff surface, such as bone or rock [39,49–53]. The joining of two different materials at an interface is a common cause of failure in many engineered parts. Nature typically generates gradient transitions, thus avoiding problematic interfaces such as weak/strong or most notably hard/soft, as shown in Figs. 3(*d*) and 3(*e*). Unlike bilayer materials, gradient materials do not possess a sharp interface and have a continuously changing composition, which helps to connect the materials to eliminate stress at the interface and endpoint stress singularity [39,54].

One gradient material is squid beak, which represents one of the hardest and stiffest organic materials. The stiff material is anchored in soft tissue and to avoid interfacial stresses predominately present in bilayer materials at the interface, a stiffness gradient over two orders of magnitude is employed (Fig. 3(*d*)) [38]. Another example is mussel byssus threads that possess gradually changing mechanical properties from soft to stiff in order to efficiently attach the mussel to the rock [33]. The proximal part of the thread is elastic, but the distal part is stiff to ensure a strong attachment to the surface. The alteration of Young's modulus in the range of 50–500 MPa can be attributed to a continuous change of composition of different collagens [39], displayed in Fig. 3(*e*).

2.3 Silk. Silk is a natural protein-based composite material [55]. Optimized for millions of years, silks are one of the strongest biomaterials with high mechanical strength, toughness, and robustness. In particular, spider dragline silk's toughness can surpass industrial materials such as Kevlar or mild steel, thanks to its high extensibility with 50–60% strain at failure [56,57]. Silk structures, such as spider webs or cocoons, also show outstanding properties: lightness and resilience. Spider webs need to be stiff enough to withstand the weight of the spider and its prey while protecting the spider and its web by absorbing energy from external loads such as wind or impacts of the preys [37]. Moreover, for a localized load such as an impact of a prey, the robustness of webs can be explained by the localized failure of sacrificial

elements of the discrete structure, instead of the complete failure of the web. This mechanism happens because of the nonlinear behavior of the spider silk [6]. In addition to the outstanding mechanical properties of silk as a material and structure, silk is biodegradable and biocompatible and could lead to numerous silk-inspired industrial applications such as: wound suture, drug delivery, and tissue regeneration [58]. The mechanical properties of silks originate from their structure and hierarchical organization, which are determined by their protein sequence and the chemical and mechanical condition during the spinning process, as shown in Fig. 4(*b*) [57,59,60].

At the nanoscale, silk fiber is a protein made of long chains of amino acids or building blocks in an ordered sequence, and dictates the folding of the protein that leads to the final molecular structure [61]. The main secondary structure motifs of spider silk are: 3_{10}-helix, crystalline β-sheet, and elastic beta-spiral region [57]. The regions rich in polyalanine fold into highly oriented β-sheet crystal, which are responsible for the high strength of silk, and are embedded in a semiamorphous glycine-rich protein domain at the origin of the extensibility of spider silk (Fig. 4(*a*)) [57,61]. Under tensile load, the β-sheet crystal oriented in the length of the fiber resist to shear failure with the cooperatively of the hydrogen bonds between the sheets [62–64].

The formation of self-assembled spider silk happens during the spinning process where a highly concentrated solution of unfolded silk protein is pulled through the spinning duct of the spider. The solution is subjected to elongation and shear flow. During this process, the pH decreases and ion exchange occurs. This process stimulates the aggregation of the proteins and encourages protein self-assembly. The shear-induced elongation aligns the proteins and stimulates the formation of hydrophobic and hydrogen bonds and consequently stiff β-sheet crystals [59,60]. The natural spinning process of silk fiber is illustrated in Fig. 4(*b*).

Lin et al. [58] have shown the critical processing conditions and design parameters of silk protein self-assembly, by investigating the evolution of the structure of synthetic silk proteins under shear flow for different ratios of hydrophobic (at the origin of the strength derived from β-sheet crystals) and hydrophilic (at the origin of the semi-amorphous phase) domains and different chain lengths, with modeling and experiments. Figure 4(*a*) shows the synthetic silk model composed of hydrophobic and hydrophilic domains. At equilibrium, the silk protein solution forms spherical micelle structures where hydrophobic domains aggregate into β-sheet crystals (Fig. 4(*c*)-ii). After shear flow, the micelles merge together into larger micelles, consequently larger β-sheet crystals

Technique name	Build speed	Curing/sintering method	Material	Material type
Stereolithography	Average	UV light	Thermoplastics (elastomers)	Liquid (photopolymer)
Selective laser sintering	Fast	High power laser (e.g., CO_2 Laser)	Nylon, polystyrene, ceramics, metals	Powder (polymer)
Fused deposition modeling	Slow	Resistive heaters	Thermoplastics such as ABS, polyamide, polycarbonate, polyethylene, polypropylene, and investment casting wax	Solid (filaments)
Inkjet printing	Slow	N/A (jet depositing)	Thermoplastics such as Polyester	Liquid

(Fig. 4(c)-iii). As shown in Fig. 4(c)-iii, only proteins with longer chains show homogeneous and continuous networks along the shear flow direction. For an optimal intermediate ratio of hydrophobic and hydrophilic domains and longer polymer chain, shear flow elongates and aligns the polymer chains from isotropic structure to anisotropic cylindrical structures, and results in robust and stronger fibers.

2.4 Hair. Hair has been an essential physical characteristic for humans and animals as they protect and insulate the body against environmental threats such as high or low temperatures, sunlight, humidity and dryness, injuries and impacts. Hair is also known for its impressive mechanical properties and very long degradation time [65]. Healthy human hair has a diameter varying between 50 and 100 μm, a Young's modulus of 2.0–3.7 GPa [66], a failure stress, and strain of approximately 117 MPa and 35%, respectively [18]. Human hair is a complex nanocomposite fiber principally composed of keratin protein, rich in cysteine amino acid residues [18]. Hair fiber has a hierarchical organization structured from alpha-helices which are twisted and form coiled–coil dimers, microfibrils consisting of 16 coiled–coils, macrofibrils formed by microfibrils, and the matrix, cellular structure to the complete hair fiber. Hair is an intermediate filament protein, main component of hair and wool, which forms microfibrils which are embedded in a sulfur-rich matrix to compose the macrofibrils, as illustrated in Fig. 5(a). The mechanical strength and durability of hair is determined by one of the main keratin protein: trichocyte keratin, which constitutes the intermediate filaments and its interaction with matrix and disulfide bonds crosslinking [65–67].

The human hair fiber is a shape memory material: it can experience a reversible phase transformation. It can reversibly convert from straight hair to curly hair [68]. The curliness of hair is independent of ethnicities, but depends on the inhomogeneity and structure of the intermediate filament protein arrangements, in the internal nanostructure of the fiber. For example, for curly hair, the proportion of matrix is higher at the inner side of the fiber [69].

The cysteine residues of the hair keratin protein produce strong covalent disulfide bonds, at the origin of the mechanical strength of hair, which crosslink the alpha-helical protein filaments together and the matrix molecules [18,70,71]. Disulfide bonds are essential for the improvement of protein stability and is an important parameter in protein folding, molecular sensing, and signaling. For example, the stability of proteins in synthetic materials can be improved by inserting cysteine amino acids in the protein sequence, which will form disulfide bonds [70]. The redox potential of the chemical microenvironment influences the stability of the disulfide bonds. Disulfide crosslinks are stronger in an oxidizing environment where they were formed, while they can be weaker and broken in the presence of reducing agents, as the energy barrier of disulfide bonds decreases in a reducing environment [72]. Disulfide crosslinks within the matrix and between the matrix molecules and microfibrils strengthen and increase the robustness of the resulting macrofilaments, by improving the cooperative deformation of the microfibrils [66], as shown in Fig. 5(b).

Simulations on a three-strand model consisting of three alpha-helical proteins connected by a cluster of disulfide crosslinks with variable geometric arrangement and strength, under tensile load as shown in Fig. 5(c), have been conducted to demonstrate the influence of molecular geometry and disulfide bond strength on the mechanical properties of the system, which can be directly related to the mechanical properties of hair fiber. It was found that strong disulfide crosslinks, found in oxidizing environment for instance, resist better external tensile load, but their cooperativeness is reduced and the system loses its original alpha-helical structure. By controlling the strength and the arrangement of the disulfide bonds, new bio-inspired structural materials can be designed for high-performance and tunable mechanical properties. One possible future engineering application would be to reduce crack propagation in fiber biomaterials by introducing weaker disulfide crosslinks, which improve ductility and toughness through cooperativity [70]. The disulfide crosslinks can be formed by inserting cysteine amino acids in the protein sequence [70] and then can be weakened by a reducing environment [72].

3 Current State of Additive Manufacturing

As seen from Sec. 2, many natural materials obtain their high performing properties through complex architectures and anisotropic structures optimized for their environment and need, built at multiple hierarchical length-scales. These designs are often difficult to replicate through traditional subtractive manufacturing methods such as using lathes and mills; instead, additive manufacturing has the intrinsic advantage to be used as a means to achieve any irregular geometric shape of complex architectures and various material properties. Additive manufacturing is an emerging technology that allows the creation of such bio-inspired materials. Whereas traditional subtractive manufacturing takes a block of material and chips away material until a desired material is obtained, additive manufacturing oftentimes involves starting with nothing and building layer-by-layer materials until a desired material is obtained. Casting, forming, molding, and machining are complex processes that involve tooling, machinery, computers, and robots. Different types of additive manufacturing are referenced in literature [73,74]. Several research groups have made efforts to 3D-print various bio-inspired composites. Here, we discuss the advantages of and basic mechanisms of 3D-printing and related techniques.

3.1 Advantages of 3D-Printing. A variety of benefits exist while using additive manufacturing. One benefit is the ability to manufacture parts with increased complexity. Additive manufacturing allows designers to selectively place material only where it is needed, allowing the creation of nature inspired materials such as cellular materials and also curving channels as needed in microfluidics. Other manufacturing processes such as metal casting and injection molding require a new mold in which to cast the part, which is not the case for additive manufacturing. The second benefit is waste reduction. Since material is added layer by layer, only the material needed for the part is used in production. The

third benefit lies in the fact that delivering parts may no longer be needed in the future; instead of shipping parts, one can ship a design file and materials and parts could be locally produced, even onsite (e.g., in construction). Designs, not products, would move around the world as files to be printed anywhere [75].

3.2 Basic Mechanisms of 3D-Printing. Currently, there are four major 3D-printing methods: stereolithography (STL), inkjet printing, selective laser sintering (SLS), and deposition modeling [76]. The limitations that exist for various additive manufacturing techniques can be categorized by build speed, curing/sintering method, and material [8,73], as summarized in Table 2.

In STL, an ultraviolet (UV) laser is used to trace the shape of the 3D object by focusing on a vat that is filled with liquid photoresin. The photoresin starts curing upon contact with the UV radiation and solidifies into the desired 3D object. STL is limited as it can only use one resin at a time, and the resins are often either epoxy-based or acrylic. The constraints in the material often result in objects that are brittle and, often, the deposited material will also shrink upon polymerization [77].

Inkjet printing, originally used for 2D applications, can be used for printing in the 3D due to the binding of powders. In 3D inkjet printing, a layer of powder is evenly placed on a stage and droplets of binding agent are printed onto the desired surface of solidification. The unbound powder is released and the process repeats for the second layer. The advantage of inkjet printing is that powder from different materials can be used to build a heterogeneous 3D model. However, the polymer glues used are often toxic and cannot be used for medical applications [78].

SLS, similar to inkjet printing, uses high-power lasers to sinter polymer powders together instead of utilizing toxic glue found in inkjet printing. Objects assembled using SLS often suffer deformation from constant heating and cooling from the laser. The precision of the printer therefore decreases, which is not optimal for applications that need high resolution such as electronic chips and biomedical implants [79].

Fused deposition modeling (FDM) is a highly used technique for 3D-printing and often deposits semimolten thermoplastic in successive layers to form the 3D structure. FDM is not limited to thermal extrusion, as materials such as ceramics and polymers can
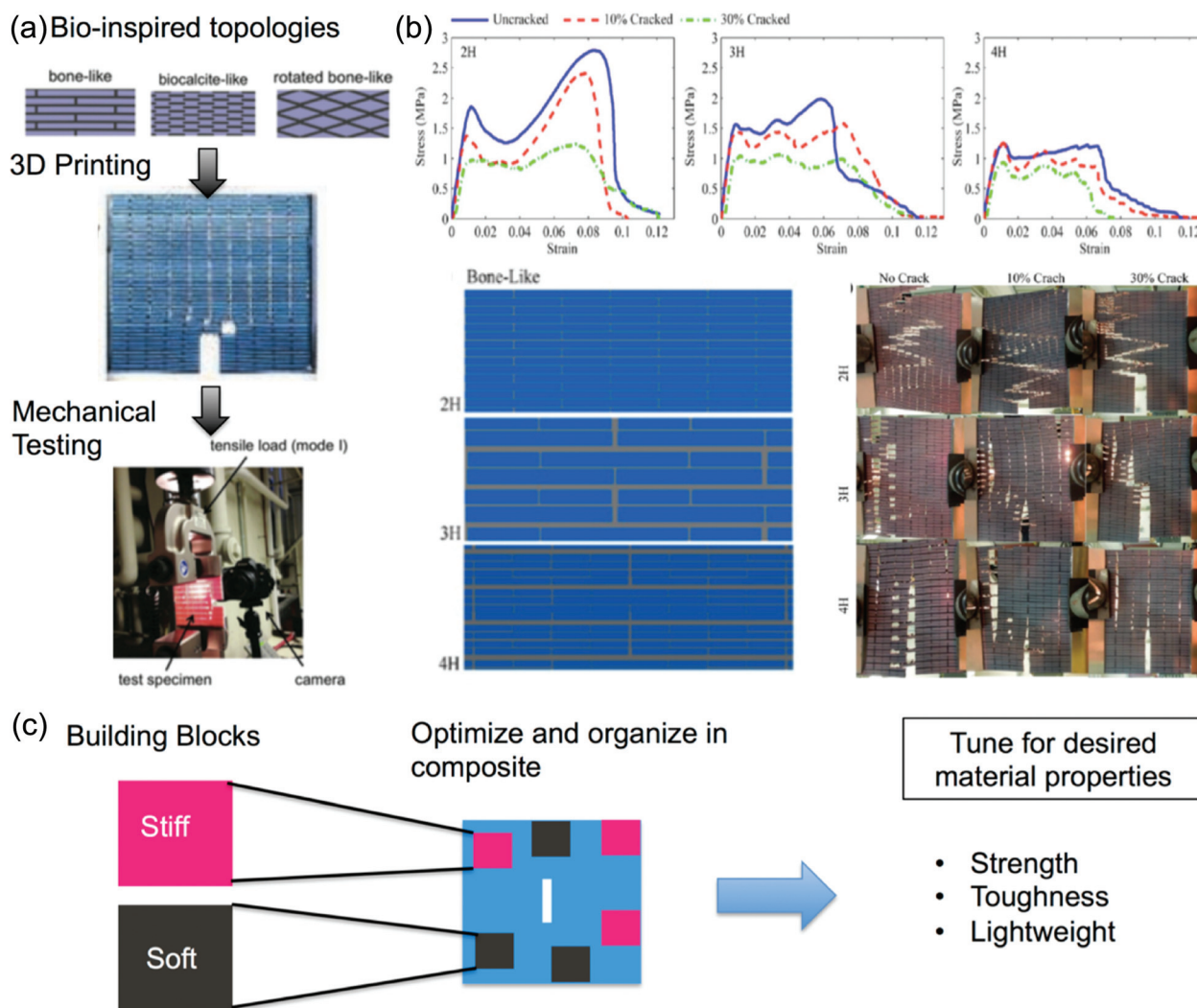

Fig. 6 (*a*) Using simple model material building blocks, Dimas et al. manufactured bio-inspired composites with 3D printing and tested the synthesized specimens to compare model predictions to experimental results [84]. Copyright 2013 by John Wiley and Sons. (*b*) Mirzaeifar et al. observed bone-like printed samples with different hierarchies. The difference between the cracked samples performance and the uncracked samples for the largest hierarchy is the smallest, indicating more defect tolerance as hierarchy increases. Crack propagation for different samples is shown and is much more delocalized for the higher hierarchy levels. Reprinted (adapted) with permission from Mirzaeifar et al. [85]. Copyright 2015 by American Chemical Society. (*c*) Optimization of composites using stiff and soft building blocks similar to natural materials.
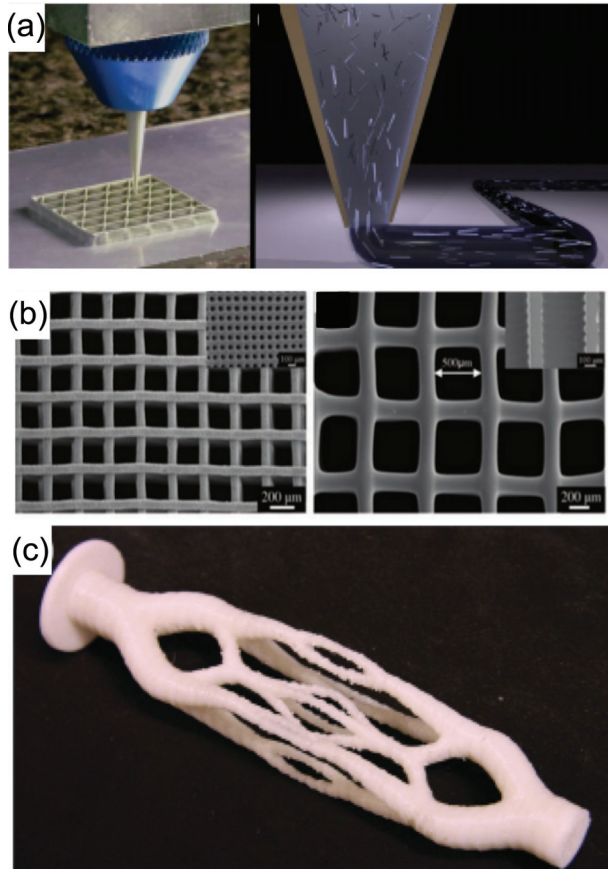
Fig. 7 (*a*) 3D printing of a triangular honeycomb composite and illustration of the progressive alignment of fillers within the nozzle during composite ink deposition. Adapted from Compton and Lewis [7]. Copyright 2014 by John Wiley and Sons. (*b*) Printed glass scaffold SEM images. Adapted from Fu et al. [90]. Copyright 2011 by John Wiley and Sons. (*c*) 3D-printed sacrificial 3D structure to make vascular template. Adapted from Gergely et al. [91]. Copyright 2015 by John Wiley and Sons.

be extruded by pressure instead of heat. However, printers that use pressure are not as accessible as printers that use heat for extrusion, which limits the materials that can be used [8,80].

Common materials for printing include acrylonitrile butadiene styrene (ABS) and polylactic acid plastic that are thermally extruded; however, materials that are ceramic, biological, and polymeric may be heat sensitive and require other modes of deposition that cannot be printed rapidly and in large-scale. Yet, several academic groups and industries are optimizing 3D-printing to resolve these constraints. In Sec. 4, several examples are given to demonstrate the usage and customization of advanced multimaterial 3D-printers for manufacturing several different materials that are biocompatible such as HA [81].

Now that we have discussed the basic mechanisms of additive manufacturing, Secs. 4 and 5 will describe various research groups' approaches to fabricating different biological composites through additive manufacturing. The paper will conclude with discussing the limitations of additive manufacturing and its future outlook.

4   Case Studies 1: 3D-Printing of Biological Composites Biomimetic Topology Designs

Composites observed in nature and used in engineering materials have a combination of vastly different materials that have superior mechanical performance compared to its base constituents [3,82,83]. Natural composites usually consist of simple

building blocks arranged in complex architectures, such as those seen in bone and abalone shells. Currently, researchers strive to mimic designs in natural composites and manufacture them using 3D-printing to design better synthetic materials. Our lab has printed composites using a multimaterial 3D printer (Stratasys Connex 3), which offers the following advantages: (1) printing complex geometries at micrometer resolutions, (2) printing a multitude of materials with varying mechanical properties, (3) printing cheaply and at a large-scale, and (4) good interfacial adhesion of the constituent materials. Using a similar multimaterial printer, Dimas et al. have studied typical biological composite topologies such as bone-like, rotated bone-like, and biocalcitelike, with a stiff and compliant phase by comparing their computational model to experimental testing on 3D-printed samples [84]. They have found that these specific topological arrangements induce significant stress and strain delocalization in their simulation and 3D-printed system [84]. In addition, Dimas et al. have found that the interfacial adhesion of the constituent materials in the printed composites is so strong that the composites do not fail at the interface, reinforcing the advancement in 3D-printing technology. This fact also agrees with their computational prediction and explains the significance of the topological arrangements for the mechanical behavior of the material [84]. These insights and techniques allow us to combine 3D-printers and computational models to create mechanically tough bio-inspired composites from simple building blocks.

Mirzaeifar et al. furthered the work to study defect tolerance of similar bio-inspired topologies with different classes of hierarchical structures [85] using multimaterial 3D-printing as a tool to validate computational results. They define defect tolerance as the ability of a material to maintain strength even under the presence of cracks, meaning the materials will be less sensitive to cracks [85]. Mirzaeifar et al. have found that in contrast to brittle base constituents of the composites, the existence of hierarchy leads to superior defect tolerant properties. Composites with more hierarchical levels dramatically improve the defect tolerance of the material (Fig. 6(*b*)). They have also compared the stress distributions in materials with different number of hierarchies in both simulation and experiments and found more uniform stress distribution in uncracked region of materials with higher hierarchy levels, providing insight about the origin of higher defect tolerance in bio-inspired materials. 3D-printing provided an avenue to quickly manufacture composites that have similar unique hierarchical structure as those seen in natural composites. Though Mirzaeifar et al. studied topologies that consisted of smaller features compared to the previous study, they were able to easily change their 3D geometry file to manufacture these samples. This fact represents the advantage of additive manufacturing compared to traditional manufacturing when it comes to studying the complex and hierarchical structures seen in biology, since basically, arbitrarily complex architectures can be manufactured and imported directly from computer models.

Further extending the work of 3D-printing of bio-inspired materials involves recent research efforts to optimize soft and stiff building blocks as seen in natural materials. Natural materials such as nacre and bone have hierarchical architectures that exhibit outstanding mechanical properties because they have evolved to survive in rain, cold, attacks from predators, and other situations. However, it begs the question if they possess the most optimized design, especially for structural applications. Natural materials have specific architectures for specific functions that may need, but it is too intricate when it comes to designing engineering materials is one question that needs to be asked. It may be better to use the soft and stiff building blocks to optimize and tune for specific mechanical properties needed for an application shown in Fig. 6(*c*). The goal of this work is to optimize the toughness of a composite by using optimization and to validate the simulation with experimental results from testing 3D-printed synthetic materials. This research can provide a proof of concept that through computational modeling, complementary material properties can
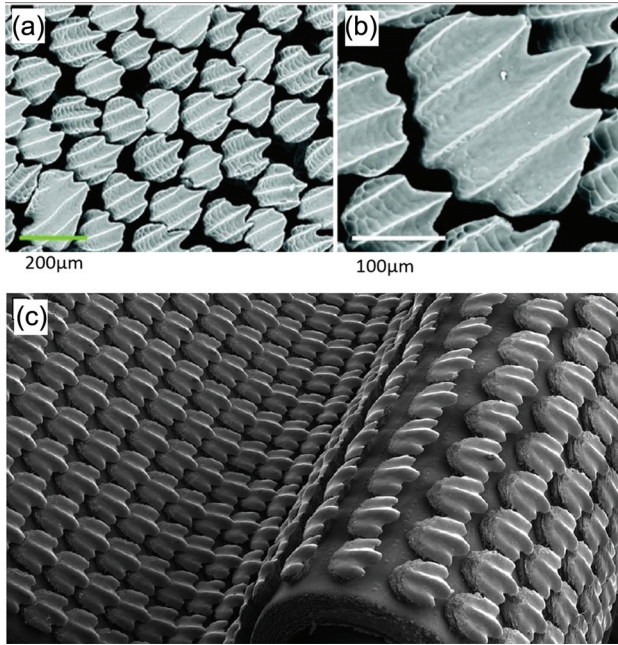
Fig. 8 SEM image of sharkskin denticles. (*a*) and (*b*) Environmental scanning electron microscope images of bonnethead shark skin surface and denticles located at its head. Adapted from Wen et al. [9]. Copyright 2014 by The Company of Biologists Ltd. (*c*) SEM image of the synthetic shark skin membrane. Adapted from Wen et al. [9]. Copyright 2014 by The Company of Biologists, Ltd. 3D-printed rigid regular shaped and spaced bio-inspired denticles fixed on a flexible membrane.

be optimized to synthesize biomimetic composites with enhanced composite morphology and superior mechanical properties.

4.1 Other 3D-Printed Materials: Cellular Structures, Gradient Materials, Among Others. Cellular materials have been known for their ability to optimize efficiently the strength to density and stiffness to density ratio. As a result, many groups look to their architecture for inspiration and strive to emulate their greatness [86–89]. Compton and Lewis in Ref. [7] have studied the manufacturing of lightweight cellular composites by using a combination of hierarchical inks and 3D-printing (Fig. 7(*a*)). Their materials have obtained Young's modulus values that are higher than those obtained by thermoplastics and photocurable resins from commercial 3D-printing companies. The growth of 3D-printing research will allow us to study more complex structures that can surpass current synthetic materials used today in engineering applications.

Anisotropic structure has been commonly observed in biological systems like wood, bone, cork, and glass sponge and has been reported to be responsible for their ability to optimize efficiently the strength to density and stiffness to density ratio. Fu et al. emulated nature's design by direct-ink-write assembling of glass scaffolds with a periodic pattern, and controlled sintering of the filaments into anisotropic constructs similar to biological materials [92] (Fig. 7(*b*)). The final product is a porous glass scaffold with a compressive strength of 136 MPa, comparable to that of cortical bone. The strength of this porous glass scaffold is also 100 times that of polymer scaffolds and 4–5 times of ceramic and glass scaffolds. This result shows the potential to 3D-print materials with properties similar to that of biological bone and superior to polymer materials.

Exoskeleton of some fish species is composed of mineralized scales that act as a protective surface from predatory threats while also allowing flexibility in axial bending and torsion [93].

Duro-Royo et al., using the armored fish exoskeleton as reference, created a computational design method to generate flexible protective surfaces [93]. They then used multimaterial 3D-printing to create prototypes with rigid and also compliant components. Using 3D-printing, they were able to test the rotation and allowable motion of their fish scale designs that can help verify their computational design method offer the potential to strengthen their bio-inspired design solution.

Gergely et al. have created bio-inspired vascular architectures using 3D-printed material as a sacrificial template (Fig. 7(*c*)). They created these templates using FDM technology. These templates are embedded in a thermosetting polymer and then removed using a thermal treatment process called vaporization of sacrificial components. This process leaves behind an inverse replica of the desired vascular design optimized by biology [91]. This group has shown the potential of using 3D-printing technology as a template to create vascular structures with their desired materials.

3D-printing of gradient materials can be applied to tissue engineering. One of the goals of functional tissue engineering is to create microenvironments that mimic the cellular and tissue complexity found in vivo by incorporating physical, chemical, temporal, and spatial gradients within engineered three-dimensional (3D) scaffolds [94]. Kalita et al. have studied how to create controlled porosity polymer–ceramic composite scaffolds using 3D-printing technology FDM and have characterized their use as bone grafts in terms of physical, mechanical, and biological properties [95]. Sherwood et al. have developed a heterogeneous osteochondral scaffold using THERIFORM 3D-printing process. They were able to vary the material composition, porosity, macroarchitecture, and mechanical properties through the scaffold structure to improve the tissue engineering process of cartilage [96].

5 Case Study 2: 3D-Printing of Biological Structures/Architectures for Functional Designs

In the design process of bio-inspired materials, 3D-printing has become an efficient method to fabricate a variety of functional materials, rapidly and precisely. Additive manufacturing is a way to investigate particular natural functional designs by rapidly manufacturing with great precision bio-inspired structures and architectures and by testing them. Although the printed structures are often orders of magnitude larger, they still provide insights into the behavior of biological material [62,97]. 3D-printing of biological and bio-inspired structures is a powerful tool to (1) investigate a specific functional design [9] and thus (2) answer the obscure biological questions when there is no or irretrievable biological data [9,98]. 3D-printing also allows a quick (3) validation of a computational model by confronting the simulations to the physical testing of the 3D-printed prototypes and make simulations an efficient predicting tool [10], and eventually (4) optimize and improve the structure of the bio-inspired material for better high-performance [99]. Finally, 3D-printing combined with behavior prediction with modeling could lead to infinite possible structural bio-inspired designs, materials, and applications with properties as good as or better than the original natural functional design.

5.1 Bio-Inspired Design for Low Drag Force in Fluid. Shark skin is composed of numerous small complex shaped denticles made of an outer enameloid layer and an inner bonelike layer (Figs. 8(*a*) and 8(*b*)). They are in direct contact with water. Shark skin performs better under propulsion and swimming conditions because of the complex 3D-shaped denticles and is also influenced by the flexibility and deformation of the skin when swimming [9] and thereby inspired scientists to create biomimetic shark skin model to investigate the role of surface roughness in the reduction of drag force. Wen, Weaver, and Lauder [9] present the first design, fabrication, and hydrodynamic testing of a synthetic, flexible, 3D-printed biomimetic shark skin membrane. The synthetic sharkskin consists of 3D-printed denticles placed on
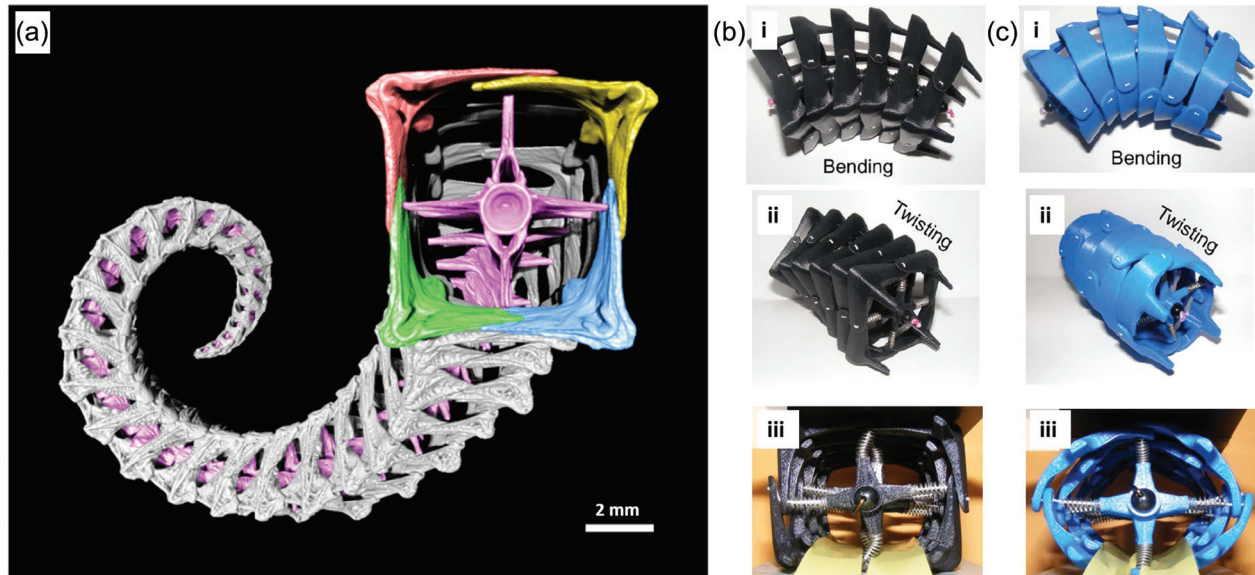
Fig. 9 Geometry and mechanical behavior of seahorse tail. Adapted from Porter et al. [98]. Copyright 2015 by The American Association for the Advancement of Science. (*a*) μCT image of seahorse tail skeleton and its cross section. The tail is composed of a series of square components constituted of four L-shaped bone plates surrounding the central vertebral column. (*b*) and (*c*) 3D-printed prototypes of seahorse (*b*) bio-inspired square tail and (*c*) hypothetical cylindrical tail, in (i) bending and (ii) twisting position. (iii) Elastic deformation just before strut disjoining of prototypes seahorse tail.

flexible membranes (Fig. 8(*c*)), which were then tested under swimming conditions, in water with a robotic flapping mechanical device. The printed denticles are ten times larger (1.5 mm) in magnitude compared to the natural ones (150 μm).

Under static drag force, meaning the membranes are immobile, 3D-printed sharkskin is subject to an increase in static drag force under high speed (but a decrease for slow speed). On the contrary, under swimming conditions, 3D-printed sharkskin has a better hydrodynamic performance compared to smooth skin membrane, as the swimming speed increases and as the swimming energy decreases. For instance, the swimming speed of the synthetic shark skins 6.6% faster than the smooth skin membrane at heave frequency of 1.5 Hz.

Understanding the role of denticles on sharkskin allows numerous design possibilities of surface roughness with enhanced hydrodynamic performance, by changing the denticles shape or pattern, for example. Synthetic biomimetic sharkskin could lead to high drag force reduced swimsuits or wetsuits.

5.2 Investigate the Biological Function of an Animal Tail. Contrarily to most animal tails, instead of being cylindrical,

seahorse tail is squared. Seahorses use their flexible tails to escape from predators by hiding themselves and to capture prey by grasping object in the sea, instead of using them to swim. Seahorse tail armor is arranged into a series of squared elements composed of four articulated L-shaped bony plates, enclosing the body, which transfer forces through muscles to the central vertebral column (Fig. 9(*a*)). To understand the role of the unusual shape of seahorse tail, Porter et al. [98] have investigated the mechanical performance of seahorse squared tail by testing 3D-printed prototypes mimicking a squared seahorse tail and a hypothetical cylindrical one for reference.

Square tail can bend as much as the cylindrical tail but only along planes parallel to the plates (cylindrical tail can bend in all directions) (Figs. 9(*b*)-i and 9(*c*)-i). On the other hand, cylindrical tail can twist twice as much as the square tail, which is a drawback for the cylindrical tail as the over-twisting can induce damage and misalignment of the internal organs (Figs. 9(*b*)-ii and 9(*c*)-ii). Besides, the excessive bending and twisting require more energy to return the tail to its resting position. Contrarily to cylinder tail, square tail assists in tail relaxation as only the square tail returns to the same linearly aligned resting position. In addition, square
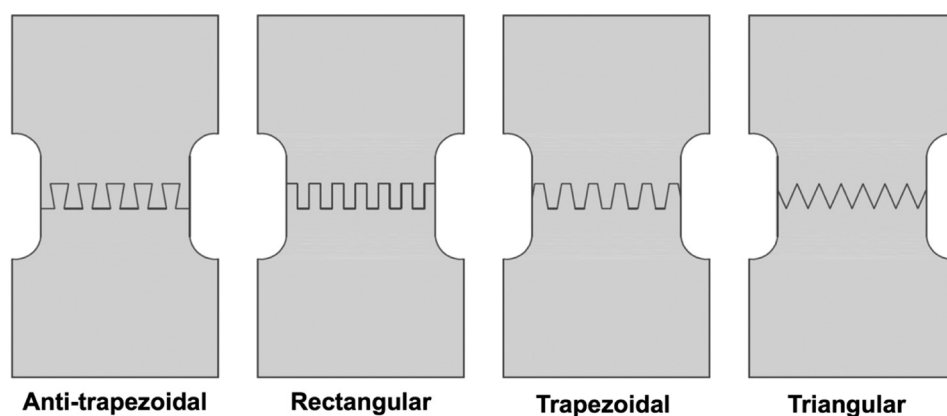

Fig. 10 Schematic of 3D-printed bio-inspired suture interface with different tailored waveforms (antitrapezoidal, rectangular, trapezoidal, and triangular) [100]
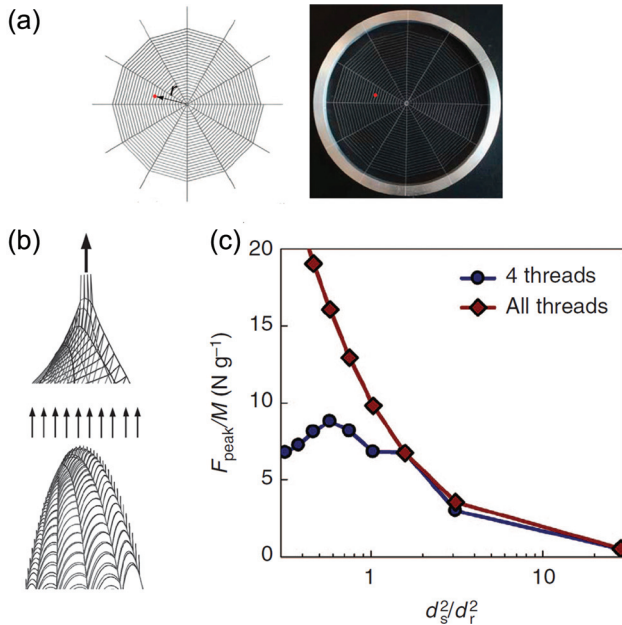
Fig. 11 Influence of material distribution on web strength under different types of loading. Adapted from Qin et al. [99]. Copyright 2015 by Nature Publishing Group. (a) Web geometry. Left: Computational model. Right: 3D-printed bio-inspired spider web. Radius of the web is $R = 50.8$ mm. (b) Snapshots of simulations of the web under (up) local load on four spiral threads and (down) homogenously distributed uniform load. (c) Plot of F_{peak}/M versus d_s^2/d_r^2, where F_{peak} is the peak force, M is the total mass of the web, d_s is the diameter of spiral threads and d_r is the diameter of radial threads. The maximum peak force occurs: (1) under local load on four spiral threads when $d_s \approx d_r$, and (2) under uniform loading when $d_s \ll d_r$.
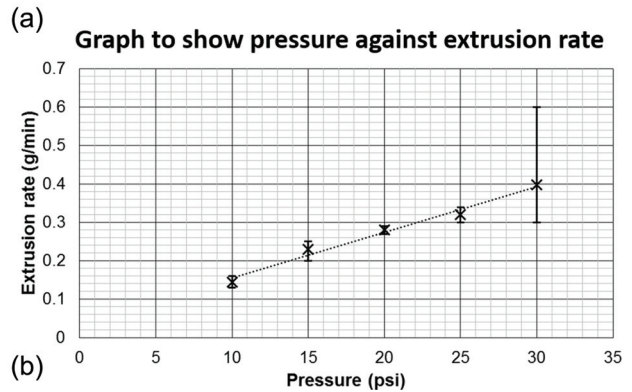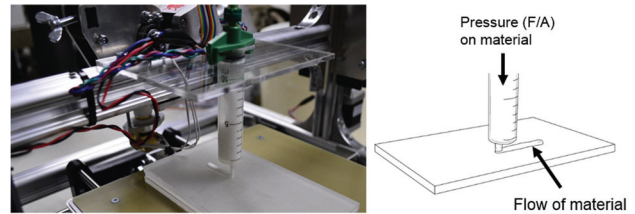

Fig. 12 (a) Photo of our HA 3D-printer, adapted for HA ink extrusion via pressurized air. Air is pushed through the top of syringe in order to extrude material out of nozzle below onto substrate, while print bed moves. The printer bed moves in the x,y-direction while the nozzle moves in the z-direction. The syringe and nozzle can easily be changed to accommodate different materials. (b) As the 3D-printer constructed in the Buehler lab uses pressure extrusion to print viscoelastic material, the flow rate for HA ink at varying pressures was recorded when the ink was loaded in a 10 cc syringe. A linear trend is observed and shows that with increasing pressure, the flow rate increases.

tails provide a better grasp of objects as they have a larger contact area and stability. Under impact and compression loading, the bone plates slide over each other (Figs. 9(b)-iii and 9(c)-iii), instead of forming plastic hinges, which is the case if the tails were constituted of one solid squared or cylindrical ring elements instead of four articulated plates. Thus, square tail performs better under impact and crushing loading, and they are stiffer, stronger, and more resilient than the cylindrical tail. Square tail shape is stiffer (3 times), stronger (4 times), and more elastic (1.5 times) [98]. Understanding the mechanics of the square tail could lead to seahorse-inspired designs which could be applied to armored system or robotics for instance. In particular, 3D-printed seahorse-inspired robots would be lighter, stronger, more flexible, and show high prehensily [98].

5.3 Validate and Model and Tailor Mechanical Behavior of Fish Suture. Suture interface is a biological geometrically structured composite interface composed of two stiff interlocking components bonded by a compliant interfacial seam in between. The particular geometries of suture interfaces show excellent mechanical properties, such as enhanced stiffness and strength and resist crack propagation. They display flexibility for adapting growth, respiration, and mobility. Suture joints are found in numerous biological materials, and their geometries can vary from minimalist design like the sutures of skull at birth to complex design like the fractal geometries of the sutures of ammonites [10,100].

Lin et al. have designed, modeled, and 3D-printed bio-inspired sutures interfaces with different suture geometries and parameters (Fig. 10) to determine their influence on stiffness, strength, and toughness [10]. The prototypes have general trapezoidal waveforms (trapezoidal, rectangular, antitrapezoidal, and triangular) printed out of stiff polymer and are bonded along the interface

with soft polymer either with a bonded tip or a nonbonded tip. By comparing the behavior of the different suture interfaces, they have shown that triangular waveforms are optimal for high stiffness, strength, and toughness and distribute uniformly stress. However, because of the interlocking geometry of the antitrapezoidal suture interface, when the tip is bonded, the performance of this suture joint is interesting as well as it shows high stiffness, strength, and toughness. The accordance of the results between experiments and simulations allows for the models to become tools for tailoring and tuning mechanical properties of suture interfaces and materials and consequently increases greatly the array of possibilities and applications, such as the application of suture joints for flexible armor. This research has shown that changing slightly the simple geometry of the suture interface can generate various different mechanical behavior [10]. Thus, depending on the mechanical performance needed, the geometries can be tailored accordingly.

5.4 Structural Optimization for the Mechanics of Spider-Web-Inspired Network. Optimized by Nature, spider webs are lightweight and show outstanding mechanical performance, in addition to the high-performance silk fibers they are composed of. They ensure simultaneously multiple functions: protect the spider and off-springs, catch preys, and sense vibrations. They are composed of very thin structural radial threads and nonstructural but more adhesive spiral threads as coated with glue beads (necessary to catch preys).

To understand in more depth and optimize the mechanical performance of spider webs, 3D-printed bioinspired synthetic elastomeric 2D spider orb webs have been designed (Fig. 11(b)), tested, and optimized for better high performance (Fig. 11(a)) [99]. Under point load, the optimal geometry is a uniform distribution of thread diameter, whereas under uniform load, structural radial
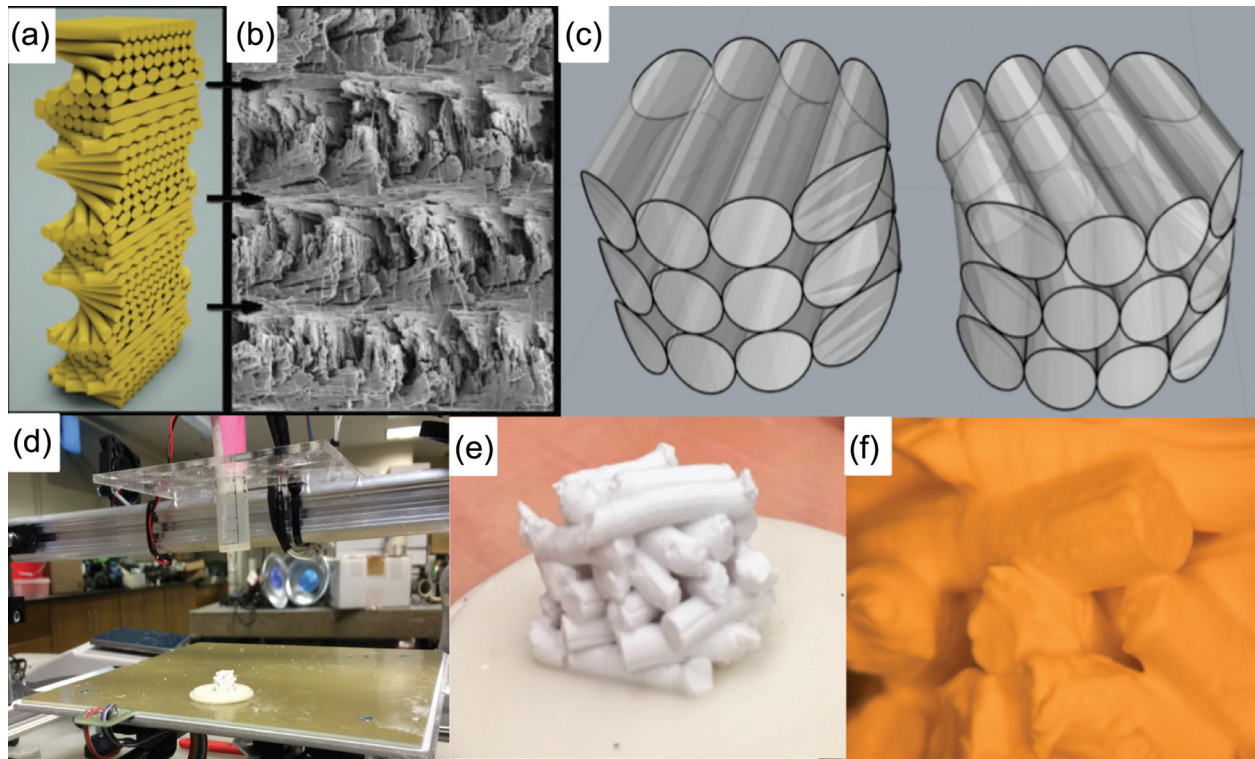
Fig. 13 (*a*) 3D-model of helicoidal structural pattern and (*b*) SEM of Mantis shrimp helicoid geometry. Adapted from Weaver et al. [53]. Copyright 2012 by The American Association for the Advancement of Science. (*c*) 3D-model of helicoid geometry constructed for finite element characterization. (*d*)–(*f*) Mantis shrimp helicoid geometry extruded using self-supporting HA ink material.

threads need to be thicker than the spiral threads, allowing sacrificial failure of spiral threads. As shown in Figs. 11(*b*) and 11(*c*), under local loading, the maximum peak force occurs when the threads have the same diameters, with slightly larger threads. Whereas under uniform loading, the maximum peak force occurs when the radial threads are significantly thicker than the spiral threads. Using the same material and in the same amount, different mechanical behaviors were obtained. Optimizing the material distribution according to loading has provided a deeper understanding on how spiders can optimize their web architecture with the same amount of silk. Learning from the experiments and simulations, new bio-inspired structures can be created and improved for better mechanical performance and lightness for a variety of engineering applications such as composite material reinforcement or scaffolding in the biomedical field.

6 Case Study 3: Limitations of 3D-Printing

While 3D-printing has allowed the evolution of various bio-inspired materials, there exist some limitations that need to be overcome for it to come to the forefront of material synthesis. The future of an ideal 3D-printing world is where we are able to print any complicated geometry with any material or materials we would like, depending on application and need. Since this is still not possible and improvements can be made, limitations are discussed in this section [8,73–75].

One universal printer limitation is the diversity of materials. Currently, only a limited number of polymers, metals, and ceramics can be used to build structures in the resolution of tens of micrometers. The selection of a material to be used in the printer depends on its ability to be a powder-based or viscoelastic material able to be extruded from a printing head. Most manufacturers create proprietary materials that they require to be the only materials used in the printer. Any violation of this requirement may cause the loss of the printer warranty and support. For 3D-printing to grow, diversity of materials must increase; one way to do this is by printing the material in a viscoelastic gel and depositing the material layer-by-layer.

The second limitation is precision. A printer's ability to print on the nanoscale should be combined with the ability to print on the macroscale. While some printing processes, such as two-photon polymerization or inkjet printing, can be used to build materials with small features on the nanoscale, they cannot be used to create large structures. In addition, printers that print macro-objects do not have the ability to print smaller ones. A more versatile printer that would allow the printing of smaller and larger features could be used for future applications in electronics [8,75].

The third limitation is the support material. Many inkjet printers use support material to fill in voids in complex geometries. Ways to remove the support material include using a water jet or manually. A better method to remove support material will be beneficial, especially in the field of microfluidics by allowing channels to be printed without support material [75].

A fourth limitation is the control of surface quality and microstructure of individual layers and segments; without this control, the reliability of the part is not high enough to ensure that the mechanical properties required for structural application are maintained. We cannot be sure that a printer that prints a certain design will produce the same prototype as another printer across the globe [75].

Our group is developing a single-material printer for HA that addresses some of these limitations. The printer is compatible with any material that can be extruded out of a nozzle with pressurized air. The architecture of the printer allows replacement parts to be easily screw-mounted on a steel frame. Figure 12(*a*) shows the printer in use. The clear acrylic attachment can easily be recut on a laser cutter to accommodate syringes of different sizes. The nozzle can also be changed in order to tune the printing diameter.

Compressed air is used to extrude the material out of a nozzle, and the print is built in a layer-by-layer method. A pressure regulator is used to control the deposition of the viscoelastic material, as shown in Fig. 12(a). Inks of HA were synthesized in our lab in order to print the mineral phase of bone for implants. Moreover, using the 3D-printer, different geometries can be printed using HA for enhanced elasticity and mechanics. The ink is synthesized in three steps: processing HA inks by calcining and ball milling, dispersing the HA and centrifuging to attain a 46 vol.% HA solution, and, finally, adding a viscosifying (4 wt.% solution phase hydroxypropylmethylcellulose) and a gelating (polyethylimine) agent. The shear thinning behavior of the HA ink allows the material to be deposited as a liquid, and hold its shape when it reaches the substrate after extrusion. It is expected that as pressure increases, the flow rate of the inks will also increase, which is observed in Fig. 12(b). Using the above flow rate vs. pressure data for HA ink, the flow rate can be easily tuned for optimal printing. Although ceramic, HA inks can be extruded at relatively low pressures in comparison to clay printing that requires 60–80 psi [101].

The nozzle in Fig. 12 is quite large and can be reduced in size with the use of a luer lock nozzle on the micron scale, thus allowing different levels of accuracy. The porosity of the material can be controlled by changing the size of the nozzle and can reach about $200\,\mu$m for HA material. The overall resolution of the printer is on the scale of millimeters, as it is restricted by the rotation of the motor.

It is hoped that material properties can be enhanced through printing patterns; this will require computational analysis of print geometries and testing for changes in material properties of prints with different patterns. A particular pattern being investigated is a helicoid pattern (as shown in Fig. 13) inspired by fiber formation in mantis shrimp clubs, which will help the overall print absorb shocks by dispersing the energy [53,102].

Another limitation to 3D-printing is the constraint on the number of materials that can be printed simultaneously. While multinozzle printers are being constructed, there are few ready for commercialization and even fewer that can use different input settings for each nozzle [103]. As materials have different flow rates and properties, extrusion has to be controlled individually and specifically for the material. Specifying the parameters of the material so the printer can print the material effectively is highly variable, and as a result, is costly and time-consuming. Given the modifiable nature of the printer, we hope to add several nozzles to print multimaterially. With multimaterial printing, we hope to better optimize function of structures.

7 Summary and Future Directions

In this article, we have discussed the properties of several biological materials such as bone, nacre, hair, and many others. Though nature has provided us a blueprint to design materials that attain higher functionality, we need to construct them with our own toolbox. As a result, we suggested and discussed the potential need for additive manufacturing to fabricate the intricate and hierarchical designs seen in nature. We have given examples of various research groups who strive to emulate designs from nature by utilizing 3D-printing technology, whether it is to make cellular structures, gradient structures, or functional designs. Next, we will discuss the future of 3D-printing and further improvements.

First, 3D-printing holds the promise of changing the manufacturing and shipping industries. In the future, companies that need to outsource their materials will be able to ship a STL file instead of an actual part. This would help to solve problems with shipping and also allow companies to have more freedom in what they wanted to create, whether it is in a unique bio-inspired structure for a turbine blade or a nacre-inspired airplane wing. For this to happen, there needs to be a better precision and reliable surface quality. The printers all around the world need to be consistent in the surface quality of the material, which is not yet accomplished. As of now in commercial printers, one part that is printed would not have the same surface finish as another part, which can be a problem when you need reliable objects such as protection armor or individual vehicle parts.

Second, 3D-printing can allow the printing of actual natural materials and use them for coating surfaces. In the future, objects can be coated with biological nacre materials that may improve mechanical properties and coating. These things cannot be explored currently due to the limitations of materials that can be printed. Currently, in commercial printers, only photopolymers that are not representative of natural materials can be printed. Hopefully, researchers who study inks that can be further combined in geometry can overcome this. This can be further improved once we have total control over the number of materials and also types of materials we can use.

Third, 3D-printing can allow us to explore the amazing natural hierarchical designs such as those in nacre and bone, and actually use those architectures to print two different types of materials to combine synthetic materials such as a polymer/metal material and a ceramic material. This would allow us to use the strong individual engineering materials to create a stronger, tougher material by emulating natural designs. In addition, 3D-printing can be used for research for testing and optimization purposes. We can, hopefully, in the future print the designs with actual materials we want to use to test and then optimize the materials and geometry to tune mechanical properties. We can currently tune properties, but only with the materials we are given.

Improvements to materials used in printing will be necessary for eventual application of 3D-printing for medical purposes; while HA inks are easily extrudable, printing collagen in conjunction with HA inks has huge scope to advance the process and present far more appropriate material properties, such as reduced brittleness. Furthermore, the integration of a well-designed material to be used as artificial collagen into printing artificial bone has potential to further ease the process of housing the scaffold in the body in the sense that the final print will be closer in structure to actual bone. Printing in more than one material is already commercially available and is typically accomplished through use of multiple nozzles, thus allowing multiple materials to be printed in unison in a single print [104]. Another technique, called the *Fill Composting Technique*, can be used. It allows integrating of two materials to design the initial print with carefully placed cavities into which the second material can later be injected. The fill composting process has been shown to enhance mechanical properties, including stiffness and yield strength, when employed in ABS and resin, thus presenting promise for use with other pairs of materials, such as artificial bone and collagen [104].

The ability to rapidly produce the appropriate 3D-model required for a given printing scenario needs improvement. As it stands, each print will require its own dedicated 3D-model to be created and virtually tested before any printing can begin. For biomedical applications, it might be useful to keep a bank of 3D-models, which can easily be modified for each specific print [76]. Similarly, a method to test or simulate how the print will perform under its intended use will need further development. In the case of printing bone scaffolds, finite element simulations will be able to determine upper bounds for the types of mechanical loads and stresses (compression, tensile, etc.) any given part of the print may experience and thus influence the print pattern design process; however, higher fidelity simulations might be necessary in some cases, such as when an finite element analysis simulation is not appropriate. Further to this, in order to expedite the print optimization process, more research will be needed on what print patterns perform well under different types of loads or stresses.

In order for the print process to accommodate more possible scenarios that require different sizes of prints, scaling the print process will be necessary [104]. Increasing or decreasing the size of printed parts will require further experimentation and testing; it is not currently obvious if it will be more beneficial to scale up the extrusion diameter and pattern or to maintain the pattern and just scale up the overall size of the object being printed. Nevertheless,

this is an area requiring further investigation. Simulation and modeling need to be used to tune the mechanical performance of the material and determine geometries that are optimal for specific functions. The pairing of 3D-printing with simulations is critical to enhanced engineering of structures. Ultimate commercialization of 3D-printing bio-inspired composites and functional materials will require further examination of costs associated with equipment and materials and further advances in the modeling process.

Acknowledgment

References

[1] Fratzl, P., 2007, "Biomimetic Materials Research: What Can we Really Learn From Nature's Structural Materials?," J. R. Soc. Interface, **4**(15), pp. 637–642.

[2] Gao, H., Ji, B., Jäger, I. L., Arzt, E., and Fratzl, P., 2003, "Materials Become Insensitive to Flaws at Nanoscale: Lessons From Nature," Proc. Natl. Acad. Sci., **100**(10), pp. 5597–5600.

[3] Bechtle, S., Ang, S. F., and Schneider, G. A., 2010, "On the Mechanical Properties of Hierarchically Structured Biological Materials," Biomaterials, **31**(25), pp. 6378–6385.

[4] Meyers, M. A., Chen, P.-Y., Lin, A. Y.-M., and Seki, Y., 2008, "Biological Materials: Structure and Mechanical Properties," Prog. Mater. Sci., **53**(1), pp. 1–206.

[5] Meyers, M. A., McKittrick, J., and Chen, P.-Y., 2013, "Structural Biological Materials: Critical Mechanics-Materials Connections," Science, **339**(6121), pp. 773–779.

[6] Cranford, S. W., Tarakanova, A., Pugno, N. M., and Buehler, M. J., 2012, "Nonlinear Material Behaviour of Spider Silk Yields Robust Webs," Nature, **482**(7383), pp. 72–76.

[7] Compton, B. G., and Lewis, J. A., 2014, "3D-Printing of Lightweight Cellular Composites," Adv. Mater., **26**(34), pp. 5930–5935.

[8] Gross, B. C., Erkal, J. L., Lockwood, S. Y., Chen, C., and Spence, D. M., 2014, "Evaluation of 3D Printing and Its Potential Impact on Biotechnology and the Chemical Sciences," Anal. Chem., **86**(7), pp. 3240–3253.

[9] Wen, L., Weaver, J. C., and Lauder, G. V., 2014, "Biomimetic Shark Skin: Design, Fabrication and Hydrodynamic Function," J. Exp. Biol., **217**(10), pp. 1656–1666.

[10] Lin, E., Li, Y., Ortiz, C., and Boyce, M. C., 2014, "3D Printed, Bio-Inspired Prototypes and Analytical Models for Structured Suture Interfaces With Geometrically-Tuned Deformation and Failure Behavior," J. Mech. Phys. Solids, **73**, pp. 166–182.

[11] Khalyfa, A., Vogt, S., Weisser, J., Grimm, G., Rechtenbach, A., Meyer, W., and Schnabelrauch, M., 2007, "Development of a New Calcium Phosphate Powder-Binder System for the 3D Printing of Patient Specific Implants," J. Mater. Sci., **18**(5), pp. 909–916.

[12] Luz, G. M., and Mano, J. F., 2009, "Biomimetic Design of Materials and Biomaterials Inspired by the Structure of Nacre," Philos. Trans. R. Soc. London A, **367**(1893), pp. 1587–1605.

[13] Bhushan, B., 2009, "Biomimetics: Lessons From Nature—An Overview," Philos. Trans. R. Soc. London A, **367**(1893), pp. 1445–1486.

[14] Downer, L., and Dockrill, P., 2008, "Whalepower Tubercle Blade Power Performance Test Report," Wind Energy Institute of Canada, Tignish, PE, Canada.

[15] Launey, M. E., Buehler, M. J., and Ritchie, R. O., 2010, "On the Mechanistic Origins of Toughness in Bone," Annu. Rev. Mater. Res., **40**(1), pp. 25–53.

[16] Jackson, A., Vincent, J., and Turner, R., 1988, "The Mechanical Design of Nacre," Proc. R. Soc. London B, **234**(1277), pp. 415–440.

[17] Barthelat, F., and Espinosa, H., 2007, "An Experimental Investigation of Deformation and Fracture of Nacre—Mother of Pearl," Exp. Mech., **47**(3), pp. 311–324.

[18] Seshadri, I. P., and Bhushan, B., 2008, "In Situ Tensile Deformation Characterization of Human Hair With Atomic Force Microscopy," Acta Mater., **56**(4), pp. 774–781.

[19] Henkel, J., Woodruff, M. A., Epari, D. R., Steck, R., Glatt, V., Dickinson, I. C., Choong, P. F., Schuetz, M. A., and Hutmacher, D. W., 2013, "Bone Regeneration Based on Tissue Engineering Conceptions—A 21st Century Perspective," Bone Res., **1**(3), pp. 216–248.

[20] Sun, J., and Bhushan, B., 2012, "Hierarchical Structure and Mechanical Properties of Nacre: A Review," RSC Adv., **2**(20), pp. 7617–7632.

[21] Currey, J., 1977, "Mechanical Properties of Mother of Pearl in Tension," Proc. R. Soc. London, Ser. B, **196**(1125), pp. 443–463.

[22] Menig, R., Meyers, M., Meyers, M., and Vecchio, K., 2000, "Quasi-Static and Dynamic Mechanical Response of Haliotis Rufescens (Abalone) Shells," Acta Mater., **48**(9), pp. 2383–2398.

[23] Gosline, J. M., Guerette, P. A., Ortlepp, C. S., and Savage, K. N., 1999, "The Mechanical Design of Spider Silks: From Fibroin Sequence to Mechanical Function," J. Exp. Biol., **202**(23), pp. 3295–3303.

[24] Weiner, S., and Wagner, H. D., 1998, "The Material Bone: Structure–Mechanical Function Relations," Annu. Rev. Mater. Sci., **28**(1), pp. 271–298.

[25] Ritchie, R. O., 2011, "The Conflicts Between Strength and Toughness," Nat. Mater., **10**(11), pp. 817–822.

[26] Dunlop, J. W., and Fratzl, P., 2010, "Biological Composites," Annu. Rev. Mater. Res., **40**(1), pp. 1–24.

[27] Tai, K., Dao, M., Suresh, S., Palazoglu, A., and Ortiz, C., 2007, "Nanoscale Heterogeneity Promotes Energy Dissipation in Bone," Nat. Mater., **6**(6), pp. 454–462.

[28] Blaiszik, B., Kramer, S., Olugebefola, S., Moore, J. S., Sottos, N. R., and White, S. R., 2010, "Self-Healing Polymers and Composites," Annu. Rev. Mater. Res., **40**(1), pp. 179–211.

[29] Einhorn, T. A., 1998, "The Cell and Molecular Biology of Fracture Healing," Clin. Orthop. Relat. Res., **355**, pp. S7–S21.

[30] Reddi, A., 1998, "Initiation of Fracture Repair by Bone Morphogenetic Proteins," Clin. Orthop. Relat. Res., **355**, pp. S66–S72.

[31] Hadjidakis, D. J., and Androulakis, I. I., 2006, "Bone Remodeling," Ann. N. Y. Acad. Sci., **1092**(1), pp. 385–396.

[32] Kickelbick, G., 2007, Hybrid Materials: Synthesis, Characterization, and Applications, Wiley, Weinheim, Germany.

[33] Qin, Z., and Buehler, M. J., 2013, "Impact Tolerance in Mussel Thread Networks by Heterogeneous Material Distribution," Nat. Commun., **4**, p. 2187.

[34] Munch, E., Launey, M. E., Alsem, D. H., Saiz, E., Tomsia, A. P., and Ritchie, R. O., 2008, "Tough, Bio-Inspired Hybrid Materials," Science, **322**(5907), pp. 1516–1520.

[35] Liu, J., Feng, X., Fryxell, G. E., Wang, L. Q., Kim, A. Y., and Gong, M., 1998, "Hybrid Mesoporous Materials With Functionalized Monolayers," Adv. Mater., **10**(2), pp. 161–165.

[36] Pedro, G., and Sanchez, C., 2006, Functional Hybrid Materials, Wiley, Weinheim, Germany.

[37] Chen, P. Y., Lin, A. Y. M., Lin, Y. S., Seki, Y., Stokes, A. G., Peyras, J., Olevsky, E. A., Meyers, M. A., and McKittrick, J., 2008, "Structure and Mechanical Properties of Selected Biological Materials," J. Mech. Behav. Biomed. Mater., **1**(3), pp. 208–226.

[38] Miserez, A., Schneberk, T., Sun, C., Zok, F. W., and Waite, J. H., 2008, "The Transition From Stiff to Compliant Materials in Squid Beaks," Science, **319**(5871), pp. 1816–1819.

[39] Claussen, K. U., Scheibel, T., Schmidt, H. W., and Giesa, R., 2012, "Polymer Gradient Materials: Can Nature Teach us New Tricks?," Macromol. Mater. Eng., **297**(10), pp. 938–957.

[40] Espinosa, H. D., Rim, J. E., Barthelat, F., and Buehler, M. J., 2009, "Merger of Structure and Material in Nacre and Bone—Perspectives on De Novo Biomimetic Materials," Prog. Mater. Sci., **54**(8), pp. 1059–1100.

[41] Ji, B., and Gao, H., 2004, "Mechanical Properties of Nanostructure of Biological Materials," J. Mech. Phys. Solids, **52**(9), pp. 1963–1990.

[42] Feng, Q., Cui, F., Pu, G., Wang, R., and Li, H., 2000, "Crystal Orientation, Toughening Mechanisms and a Mimic of Nacre," Mater. Sci. Eng. C, **11**(1), pp. 19–25.

[43] Song, F., Soh, A., and Bai, Y., 2003, "Structural and Mechanical Properties of the Organic Matrix Layers of Nacre," Biomaterials, **24**(20), pp. 3623–3631.

[44] Wang, R., and Gupta, H. S., 2011, "Deformation and Fracture Mechanisms of Bone and Nacre," Annu. Rev. Mater. Res., **41**(1), pp. 41–73.

[45] Barthelat, F., 2010, "Nacre From Mollusk Shells: A Model for High-Performance Structural Materials," Bioinspiration Biomimetics, **5**(3), p. 035001.

[46] Brümmer, F., Pfannkuchen, M., Baltz, A., Hauser, T., and Thiel, V., 2008, "Light Inside Sponges," J. Exp. Mar. Biol. Ecol., **367**(2), pp. 61–64.

[47] Gilbert, S. F., Loredo, G. A., Brukman, A., and Burke, A. C., 2001, "Morphogenesis of the Turtle Shell: The Development of a Novel Structure in Tetrapod Evolution," Evol. Dev., **3**(2), pp. 47–58.

[48] Scheyer, T., 2007, "Comparative Bone Histology of the Turtle Shell (Carapace and Plastron) Implications for Turtle Systematics, Functional Morphology and Turtle Origins," Ph.D. dissertation, Institut für Paläontologie, Rheinische Friedrich-Wilhelms-Universität, Bonn, Germany.

[49] Wu, X., Jiang, P., Chen, L., Zhang, J., Yuan, F., and Zhu, Y., 2014, "Synergetic Strengthening by Gradient Structure," Mater. Res. Lett., **2**(4), pp. 185–191.

[50] Phillips, J. E., Burns, K. L., Le Doux, J. M., Guldberg, R. E., and García, A. J., 2008, "Engineering Graded Tissue Interfaces," Proc. Natl. Acad. Sci., **105**(34), pp. 12170–12175.

[51] Wu, X., Jiang, P., Chen, L., Yuan, F., and Zhu, Y. T., 2014, "Extraordinary Strain Hardening by Gradient Structure," Proc. Natl. Acad. Sci., **111**(20), pp. 7197–7201.

[52] Qin, Z., and Buehler, M. J., 2014, "Molecular Mechanics of Mussel Adhesion Proteins," J. Mech. Phys. Solids, **62**, pp. 19–30.

[53] Weaver, J. C., Milliron, G. W., Miserez, A., Evans-Lutterodt, K., Herrera, S., Gallana, I., Mershon, W. J., Swanson, B., Zavattieri, P., and DiMasi, E., 2012, "The Stomatopod Dactyl Club: A Formidable Damage-Tolerant Biological Hammer," Science, **336**(6086), pp. 1275–1280.

[54] Udupa, G., Rao, S. S., and Gangadharan, K., 2014, "Functionally Graded Composite Materials: An Overview," Procedia Mater. Sci., **5**, pp. 1291–1299.

[55] Hardy, J. G., and Scheibel, T. R., 2010, "Composite Materials Based on Silk Proteins," Prog. Polym. Sci., **35**(9), pp. 1093–1115.

[56] Giesa, T., Arslan, M., Pugno, N. M., and Buehler, M. J., 2011, "Nanoconfinement of Spider Silk Fibrils Begets Superior Strength, Extensibility, and Toughness," Nano Lett., **11**(11), pp. 5038–5046.

[57] Tokareva, O., Jacobsen, M., Buehler, M., Wong, J., and Kaplan, D. L., 2014, "Review: Structure–Function–Property–Design Interplay in Biopolymers: Spider Silk," Acta Biomater., **10**(4), pp. 1612–1626.

[58] Lin, S., Ryu, S., Tokareva, O., Gronau, G., Jacobsen, M. M., Huang, W., Rizzo, D. J., Li, D., Staii, C., Pugno, N. M., Wong, J. Y., Kaplan, D. L., and Buehler, M. J., 2015, "Predictive Modelling-Based Design and Experiments for Synthesis and Spinning of Bioinspired Silk Fibres," Nat. Commun., **6**, pp. 6892–6892.

[59] Rammensee, S., Slotta, U., Scheibel, T., and Bausch, A. R., 2008, "Assembly Mechanism of Recombinant Spider Silk Proteins," Proc. Natl. Acad. Sci., **105**(18), pp. 6590–6595.

[60] Hardy, J. G., Römer, L. M., and Scheibel, T. R., 2008, "Polymeric Materials Based on Silk Proteins," Polymer, **49**(20), pp. 4309–4327.

[61] Tarakanova, A., and Buehler, M. M. M. E., 2012, "A Materiomics Approach to Spider Silk: Protein Molecules to Webs," J. Miner. Met. Mater. Soc., **64**(2), pp. 214–225.

[62] Qin, Z., Dimas, L., Adler, D., Bratzel, G., and Buehler, M. J., 2014, "Biological Materials by Design," J. Phys.: Condens. Matter, **26**(7), p. 073101.

[63] Qin, Z., and Buehler, M. J., 2012, "Cooperativity Governs the Size and Structure of Biological Interfaces," J. Biomech., **45**(16), pp. 2778–2783.

[64] Keten, S., Xu, Z., Ihle, B., and Buehler, M. J., 2010, "Nanoconfinement Controls Stiffness, Strength and Mechanical Toughness of β-Sheet Crystals in Silk," Nat. Mater., **9**(4), pp. 359–367.

[65] Matsunaga, R., Abe, R., Ishii, D., Watanabe, S.-I., Kiyoshi, M., Nöcker, B., Tsuchiya, M., and Tsumoto, K., 2013, "Bidirectional Binding Property of High Glycine–Tyrosine Keratin-Associated Protein Contributes to the Mechanical Strength and Shape of Hair," J. Struct. Biol., **183**(3), pp. 484–494.

[66] Chou, C.-C., Lepore, E., Antonaci, P., Pugno, N., and Buehler, M. J., 2015, "Mechanics of Trichocyte Alpha-Keratin Fibers: Experiment, Theory, and Simulation," J. Mater. Res., **30**(1), pp. 26–35.

[67] Chou, C.-C., and Buehler, M. J., 2012, "Structure and Mechanical Properties of Human Trichocyte Keratin Intermediate Filament Protein," Biomacromolecules, **13**(11), pp. 3522–3532.

[68] Quinlan, R. A., Bromley, E. H., and Pohl, E., 2015, "A Silk Purse From a Sow's Ear—Bioinspired Materials Based on α-Helical Coiled Coils," Curr. Opin. Cell Biol., **32**, pp. 131–137.

[69] Kajiura, Y., Watanabe, S., Itou, T., Nakamura, K., Iida, A., Inoue, K., Yagi, N., Shinohara, Y., and Amemiya, Y., 2006, "Structural Analysis of Human Hair Single Fibres by Scanning Microbeam SAXS," J. Struct. Biol., **155**(3), pp. 438–444.

[70] Chou, C.-C., and Buehler, M. J., 2012, "Molecular Mechanics of Disulfide Bonded Alpha-Helical Protein Filaments," BioNanoScience, **3**(1), pp. 85–94.

[71] McKittrick, J., Chen, P. Y., Bodde, S. G., Yang, W., Novitskaya, E. E., and Meyers, M. A., 2012, "The Structure, Functions, and Mechanical Properties of Keratin," JOM, **64**(4), pp. 449–468.

[72] Keten, S., Chou, C.-C., van Duin, A. C. T., and Buehler, M. J., 2012, "Tunable Nanomechanics of Protein Disulfide Bonds in Redox Microenvironments," J. Mech. Behav. Biomed. Mater., **5**(1), pp. 32–40.

[73] Gibson, I., Rosen, D. W., and Stucker, B., 2010, *Additive Manufacturing Technologies*, Springer, New York.

[74] Gao, W., Zhang, Y., Ramanujan, D., Ramani, K., Chen, Y., Williams, C. B., Wang, C. C., Shin, Y. C., Zhang, S., and Zavattieri, P. D., 2015, "The Status, Challenges, and Future of Additive Manufacturing in Engineering," Comput. Aided Des., **69**, pp. 65–89.

[75] Campbell, T., Williams, C., Ivanova, O., and Garrett, B., 2011, "Could 3D Printing Change the World," *Technologies, Potential, and Implications of Additive Manufacturing*, Atlantic Council, Washington, DC.

[76] Bhatia, S. K., and Sharma, S., 2014, "3D-Printed Prosthetics Roll Off the Presses," Chem. Eng. Prog., **110**(5), pp. 28–33.

[77] Melchels, F. P. W., Feijen, J., and Grijpma, D. W., 2010, "A Review on Stereolithography and Its Applications in Biomedical Engineering," Biomaterials, **31**(24), pp. 6121–6130.

[78] Doraiswamy, A., Dunaway, T. M., Wilker, J. J., and Narayan, R. J., 2009, "Inkjet Printing of Bioadhesives," J. Biomed. Mater. Res., **89B**(1), pp. 28–35.

[79] Kumar, S., 2003, "Selective Laser Sintering: A Qualitative and Objective Approach," JOM, **55**(10), pp. 43–47.

[80] Miller, J. S., Stevens, K. R., Yang, M. T., Baker, B. M., Nguyen, D.-H. T., Cohen, D. M., Toro, E., Chen, A. A., Galie, P. A., and Yu, X., 2012, "Rapid Casting of Patterned Vascular Networks for Perfusable Engineered Three-Dimensional Tissues," Nat. Mater., **11**(9), pp. 768–774.

[81] Wang, H., Li, Y., Zuo, Y., Li, J., Ma, S., and Cheng, L., 2007, "Biocompatibility and Osteogenesis of Biomimetic Nano-Hydroxyapatite/Polyamide Composite Scaffolds for Bone Tissue Engineering," Biomaterials, **28**(22), pp. 3338–3348.

[82] Landel, R. F., and Nielsen, L. E., 1993, *Mechanical Properties of Polymers and Composites*, CRC Press, New York.

[83] Thostenson, E. T., Ren, Z., and Chou, T.-W., 2001, "Advances in the Science and Technology of Carbon Nanotubes and Their Composites: A Review," Compos. Sci. Technol., **61**(13), pp. 1899–1912.

[84] Dimas, L. S., Bratzel, G. H., Eylon, I., and Buehler, M. J., 2013, "Tough Composites Inspired by Mineralized Natural Materials: Computation, 3D printing, and Testing," Adv. Funct. Mater., **23**(36), pp. 4629–4638.

[85] Mirzaeifar, R., Dimas, L. S., Qin, Z., and Buehler, M. J., 2015, "Defect-Tolerant Bioinspired Hierarchical Composites: Simulation and Experiment," ACS Biomater. Sci. Eng., **1**(5), pp. 295–304.

[86] Gibson, L., Ashby, M., Schajer, G., and Robertson, C., 1982, "The Mechanics of Two-Dimensional Cellular Materials," Proc. R. Soc. London A, **382**(1782), pp. 25–42.

[87] Freyman, T., Yannas, I., and Gibson, L., 2001, "Cellular Materials as Porous Scaffolds for Tissue Engineering," Prog. Mater. Sci., **46**(3), pp. 273–282.

[88] Gibson, L., 1989, "Modelling the Mechanical Behavior of Cellular Materials," Mater. Sci. Eng. A, **110**, pp. 1–36.

[89] Christensen, R. M., 2000, "Mechanics of Cellular and Other Low-Density Materials," Int. J. Solids Struct., **37**(1), pp. 93–104.

[90] Fu, Q., Saiz, E., and Tomsia, A. P., 2011, "Bioinspired Strong and Highly Porous Glass Scaffolds," Adv. Funct. Mater., **21**(6), pp. 1058–1063.

[91] Gergely, R. C., Pety, S. J., Krull, B. P., Patrick, J. F., Doan, T. Q., Coppola, A. M., Thakre, P. R., Sottos, N. R., Moore, J. S., and White, S. R., 2015, "Multidimensional Vascularized Polymers Using Degradable Sacrificial Templates," Adv. Funct. Mater., **25**(7), pp. 1043–1052.

[92] Fu, Q., Saiz, E., and Tomsia, A. P., 2011, "Direct Ink Writing of Highly Porous and Strong Glass Scaffolds for Load-Bearing Bone Defects Repair and Regeneration," Acta Biomater., **7**(10), pp. 3547–3554.

[93] Duro-Royo, J., Zolotovsky, K., Mogas-Soldevila, L., Varshney, S., Oxman, N., Boyce, M. C., and Ortiz, C., 2015, "MetaMesh: A Hierarchical Computational Model for Design and Fabrication of Biomimetic Armored Surfaces," Comput. Aided Des., **60**, pp. 14–27.

[94] Sant, S., Hancock, M. J., Donnelly, J. P., Iyer, D., and Khademhosseini, A., 2010, "Biomimetic Gradient Hydrogels for Tissue Engineering," Can. J. Chem. Eng., **88**(6), pp. 899–911.

[95] Kalita, S. J., Bose, S., Hosick, H. L., and Bandyopadhyay, A., 2003, "Development of Controlled Porosity Polymer–Ceramic Composite Scaffolds Via Fused Deposition Modeling," Mater. Sci. Eng. C, **23**(5), pp. 611–620.

[96] Sherwood, J. K., Riley, S. L., Palazzolo, R., Brown, S. C., Monkhouse, D. C., Coates, M., Griffith, L. G., Landeen, L. K., and Ratcliffe, A., 2002, "A Three-Dimensional Osteochondral Composite Scaffold for Articular Cartilage Repair," Biomaterials, **23**(24), pp. 4739–4751.

[97] Wegst, U. G. K., Bai, H., Saiz, E., Tomsia, A. P., and Ritchie, R. O., 2015, "Bioinspired Structural Materials," Nat. Mater., **14**(1), pp. 23–36.

[98] Porter, M. M., Adriaens, D., Hatton, R. L., Meyers, M. A., and McKittrick, J., 2015, "Why the Seahorse Tail is Square," Science, **349**(6243), p. aaa6683.

[99] Qin, Z., Compton, B. G., Lewis, J. A., and Buehler, M. J., 2015, "Structural Optimization of 3D-Printed Synthetic Spider Webs for High Strength," Nat. Commun., **6**, pp. 7038–7038.

[100] Li, Y., Ortiz, C., and Boyce, M. C., 2011, "Stiffness and Strength of Suture Joints in Nature," Phys. Rev. E, **84**(6), p. 062904.

[101] Lewis, J. A., Smay, J. E., Stuecker, J., and Cesarano, J., 2006, "Direct Ink Writing of Three-Dimensional Ceramic Structures," J. Am. Ceram. Soc., **89**(12), pp. 3599–3609.

[102] Schechter, E., 2014, "Mantis Shrimp Spending Delivers Surprising Payoff," Aerosp. Am., **52**(6), pp. 8–11.

[103] Kranz, S., 2013, "Multinozzle Printheads for 3D Printing of Viscoelastic Inks," M.S. thesis, University of Illinois at Urbana-Champaign, Champaign, IL.

[104] Belter, J. T., and Dollar, A. M., 2015, "Strengthening of 3D Printed Fused Deposition Manufactured Parts Using the Fill Compositing Technique," PLoS ONE, **10**(4), p. e0122915.